

Chaotic Attractors with Discrete Planar Symmetries

NATHAN C. CARTER
RR6 Box 6538, Moscow, PA 18444, USA
ncarter@epix.net

RICHARD L. EAGLES
403 Duncan Lane, Hampstead, MD 21074, USA
eaglesr@lafayette.edu

STEPHEN M. GRIMES
6690 Nicoll Dr., N. Ridgeville, OH 44039, USA
grimes@bucknell.edu

ANDREW C. HAHN
RD 1 Box 1794, Saylorsburg, PA 18353, USA
hahna@lafayette.edu

CLIFFORD A. REITER
Department of Mathematics, Lafayette College, Easton, PA 18042, USA
reiterc@lafayette.edu

Abstract – Chaotic behavior is known to be compatible with symmetry and illustrations are constructed using functions equivariant with respect to the desired symmetries. Earlier investigations determined families of equivariant functions for a few of the discrete symmetry groups in the plane; those results are extended to all the discrete symmetry groups of the plane. This includes consideration of the all the frieze and two-dimensional crystallographic groups.

1. INTRODUCTION

Nontrivial attractors that arise from the iteration of systems have appeared in a great variety of theoretic and applied contexts. One of the most famous attractors is the Lorenz attractor [1] that arose from a model of weather; that attractor is in three space and has no apparent symmetries. Other systems have been noted to have a great deal of inherent symmetry even while exhibiting chaotic behavior. For example, the patterned flows in Courent-Taylor systems [2] have simultaneous symmetry and turbulence. Patterns arising naturally, whether they are stripes and spot formations in a biological context or x-ray diffraction patterns, are intriguing because they suggest both randomness and hidden patterns [3,4]. The

simultaneous sense of symmetry and the bizarre was used by the artist M. C. Escher, who often took advantage of frieze and crystallographic symmetries [5]; indeed, he had significant interaction with the crystallographers of his day. General introductions to symmetry include Stewart and Golubitsky [2] and Weyl [6]. Thompson's [7] classic text on the symmetry of physical forms includes Harold Edgerton's example "an instantaneous photograph of a 'splash' of milk" which has dramatic symmetry. That text also discusses the shapes and forms of many living things. Grünbaum and Shepard give a near encyclopedic discussion of patterns in the plane [8].

We can create chaotic attractors by choosing a family of maps in the plane, randomly choosing the coefficients for the terms as parameters and testing whether the Ljapunov exponent is indicative of chaotic behavior. Monte Carlo searches through parameter space yield the desired illustrations of attractors and these will have the desired symmetry if our family of maps possesses suitable properties. Figure 1 shows a nontrivial chaotic attractor with no apparent symmetry that was constructed from such a quadratic map in \mathfrak{R}^2 . Figure 2 shows an attractor with cyclic 10-fold symmetry and Figure 3 shows an attractor with dihedral 10-fold symmetry; note the dihedral symmetry also includes reflections through 10 central lines. Field and Golubitsky [9, 10] discuss classes of polynomial maps that can be used to create attractors with these symmetries. They also discuss and give illustrations of attractors with the symmetry of four of the crystallographic groups. Attractors with the symmetry of the cube [11], n -cube [12] and tetrahedron [13] have also been studied.

The discrete symmetry groups in the plane are well known to consist of the identity, two infinite families of rotational groups (cyclic and dihedral), seven frieze groups that include one independent translation each and 17 crystallographic groups that include two independent translations each [8]. Amazingly, the 230 crystallographic groups in three space were enumerated before the planar groups [8]. In the next section we look at some of the details of the maps used to create attractors with trivial and rotational symmetry in order to set the stage for our discussion of attractors with frieze and crystallographic symmetry that appears in Sections 3 and 4. For now we note we found it convenient to use three dimensional tensors to represent the parameter space. One dimension of the tensor corresponds to the pair of output coordinates and the others correspond either to a power series or a fourier series. Roughly speaking, the number of independent translations determine the number of axes dedicated to fourier series. Specific symmetries constrain the parameters and in many cases we must use special techniques to maintain equivariance with

a truncated series.

2. GROUPS WITHOUT TRANSLATION

Quadratic and higher degree functions of one variable can exhibit chaotic behavior. For example, the logistic map is a quadratic map for which this can be observed and sometimes proven. It is natural to look at two variable quadratic or higher degree maps as a potential source of chaotic behavior. Sprott [14] has done this using the Ljapunov exponent [15, 16] as a selection device. In practice one might speed up the selection process using genetic algorithms [17] but we found Monte-Carlo searches based on the lack of periodicity, lack of collinearity, and well behaved Ljapunov exponent sufficient. In some cases we also tried to select according to boundedness of each component of the complement of the attractor. Sometimes the attractor can degenerate; see [18,19] for the theory of admissible subgroups.

We may represent a degree 2 map $f_A : \mathbb{R}^2 \rightarrow \mathbb{R}^2$ by

Table I Coefficients of a Quadratic Map on the Plane

$$f_A \begin{pmatrix} x \\ y \end{pmatrix} = \langle 1, x, x^2 \rangle \bullet A \bullet \langle 1, y, y^2 \rangle = \sum_{\substack{0 \leq i \leq 2 \\ 0 \leq k \leq 2}} \begin{pmatrix} a_{i0k} x^i y^k \\ a_{i1k} x^i y^k \end{pmatrix}$$

$A_0 =$	1 0 0
	4 0 0
	2 0 0
	0 5 6
	3 0 0
	0 0 0

where $A = (a_{ijk})$ is a three dimensional array with indices bounded by $0 \leq i \leq 2, 0 \leq j \leq 1, 0 \leq k \leq 2$. Note that the indices of the coefficient a_{ijk} are such

that i corresponds to the power of x , j specifies the output coordinate, and k corresponds to the power of y . For example,

$f_{A_0} \begin{pmatrix} x \\ y \end{pmatrix} = \begin{pmatrix} 1 + 2x + 3x^2 \\ 4 + 5xy + 6xy^2 \end{pmatrix}$ corresponds to the three dimensional array shown in Table I.

Figure 1 was generated by such a function where the entries in the array were randomly selected between ± 1 . A Monte Carlo search for Ljapunov exponents between 0.05 and 0.6 was done and the figure was selected for its apparent lack of symmetry. In that figure pixels visited few times are colored in red while pixels visited more times are colored with a color with a higher hue value. The color contrast was optimized using a cumulative distribution with a logarithmic bias on frequencies, thus red appears more frequently. We will use the same scheme in general but will vary the starting hue for variety.

In order to generate attractors with specified symmetries we need functions $f: \mathfrak{R}^2 \rightarrow \mathfrak{R}^2$ that preserve those symmetries in a certain manner. In particular, a function f is said to be *equivariant* with respect to a group of symmetries if for all σ in that group of symmetries and $X \in \mathfrak{R}^2$ $f(\sigma(X)) = \sigma(f(X))$. For example, if σ is a rotation and f is σ -equivariant, then the iterates of the rotation of a point are the same as the rotation of the iterates of the point. This means that the attractor associated with f should have the desired symmetries. It is possible that the attractor has only the symmetry when initial point averaging is done; however, in practice, transitive attractors occur and illustrations can be constructed using these maps. Moreover, it is easy to verify that if a map is equivariant with respect to the generators of a symmetry group then it is equivariant with respect to all the elements of the group. Thus, we need only verify equivariance with respect to generators.

The theory of which polynomial maps have n -fold rotational and n -fold dihedral symmetry is given in [9]. A truncated form for these maps can be written in complex coordinates as $F(z) = (\lambda + \omega i + \alpha z \bar{z} + \beta \operatorname{Re}(z^n))z + \gamma \bar{z}^{n-1}$ where $\omega = 0$ corresponds to dihedral symmetry. Higher degree truncations can be used [20] and these maps can be put into the form of the three dimensional array described above but we are content to leave them in the given form and turn to a discussion of the frieze groups.

3. FRIEZE GROUPS

The frieze group with the least amount of symmetry is denoted p111; it has one independent direction of translation and no other symmetry. Since fourier series are often described in terms of functions that have period 2π we are interested in maps $f: \mathfrak{R}^2 \rightarrow \mathfrak{R}^2$ that are equivariant with respect to $\sigma(x, y) = (x + 2\pi, y)$. Here we have written pairs in \mathfrak{R}^2 as a row instead of a column and we will use both notations freely. Note we take our translations along the x -axis for the frieze groups. Fourier series can be used to represent smooth enough functions with period 2π . Thus we expect any function of x and y that is periodic in x and smooth enough will have the form

$$b_0(y) + \sum_{n=1}^{\infty} (b_n(y) \cos(nx) + c_n(y) \sin(nx))$$

where the coefficient functions have power series expansions in y . We take our functions to be truncated fourier series in x and truncated power series expansions in y yielding the form:

$$g_A \begin{pmatrix} x \\ y \end{pmatrix} = \langle 1, \cos(x), \cos(2x), \sin(x), \sin(2x) \rangle \bullet A \bullet \langle 1, y, y^2 \rangle \pmod{\begin{pmatrix} 2\pi \\ \infty \end{pmatrix}}$$

where A is a 5 by 2 by 3 array. The entries of this array, a_{ijk} , are such that i represents the index in the fourier terms, j indicates the output coordinate, and k indicates the power of y . Note we reduce modulo 2π in the x coordinate and do not reduce the y coordinate. We easily verify that these functions are equivariant with respect to this model of p111. Subsequent Monte-Carlo searches for attractors lead to images such as Figure 4. This figure contains sweeps and swirls repeated with period 2π as desired.

To induce symmetries in addition to translational, we impose restrictions on our family of functions or modify them in some way. The p112 symmetry group contains two-fold rotations (180°). In order to create this symmetry we require equivariance with respect to $\sigma(x,y)=(-x,-y)$. The equivariance conditions means that $g_A(\sigma(x,y))=\sigma(g_A(x,y))$. This implies

$$-(\langle I, \cos(x), \cos(2x), \sin(x), \sin(2x) \rangle \bullet A \bullet \langle I, y, y^2 \rangle)$$

which means

$$a_{000} + a_{001}(-y) + a_{002}(-y)^2 + a_{100}\cos(-x) + a_{101}(-y)\cos(-x) + \dots = \\ -a_{000} - a_{001}y - a_{002}y^2 - a_{100}\cos(x) - a_{101}y\cos(x) + \dots$$

and

$$a_{010} + a_{011}(-y) + a_{012}(-y)^2 + a_{110}\cos(-x) + a_{111}(-y)\cos(-x) + \dots = \\ -a_{010} - a_{011}y - a_{012}y^2 - a_{110}\cos(x) - a_{111}y\cos(x) + \dots$$

where a_{ijk} are the entries in the array A . Note that we have two separate equations, corresponding to the two coordinates of the maps. Simplifying and equating like terms requires that $a_{000} = -a_{000}$, $a_{001} = a_{001}$, $a_{002} = -a_{002}$, $a_{100} = -a_{100}$, $a_{101} = a_{101}$, $a_{102} = -a_{102}$,... This means sixteen of our parameters must be zero and the other fourteen are unconstrained. This allows us to limit our family of functions to those that have the desired symmetry simply by creating a mask of our array A . We can now write our family of functions for p112 as

$g_{A^*M_{p112}}\begin{pmatrix} x \\ y \end{pmatrix}$, where M_{p112} is the array mask in Table II. Note A^*M_{p112} is an elementwise

product of the matrices; this forces some of the random entries to become zero creating the desired symmetry. Note again, the result is modulo 2π in the x coordinate. Figure 5 exhibits the p112 symmetry, and results from Monte-Carlo searches. Notice this image has translations and a clear non-trivial rotation.

The frieze group pm11 has lines of symmetry perpendicular to the axis of translation. We can obtain these lines of symmetry by requiring equivariance with respect to $\sigma(x,y)=(-x,y)$. We then use an analysis similar to that used for the p112 frieze group. Thus the family of functions $g_{A^*M_{pm11}}\begin{pmatrix} x \\ y \end{pmatrix}$ with mask M_{pm11} as seen in Table II has the desired symmetry.

Figure 6 is an example of a frieze with this type of symmetry. Notice the two lines of reflection in the fundamental motif, with the second implied by the first in accordance with the periodicity.

The symmetry group $p1m1$ is characterized by a line of reflection parallel to the direction of translation. That is, we require equivariance with respect to $\sigma(x,y)=(x,-y)$ and obtain functions of the form $g_{A^*M_{p1m1}}\left(\begin{matrix} x \\ y \end{matrix}\right)$, with mask M_{p1m1} , as can be seen in Table II. Figure 7 is an image representative of this group.

Table II Array Masks for p112, pm11, p1m1, and p1a1.

p112	pm11	p1m1	p1a1
0 1 0	0 0 0	1 0 1	1 0 1
0 1 0	1 1 1	0 1 0	0 1 0
0 1 0	0 0 0	1 0 1	0 1 0
0 1 0	1 1 1	0 1 0	1 0 1
0 1 0	0 0 0	1 0 1	1 0 1
0 1 0	1 1 1	0 1 0	0 1 0
1 0 1	1 1 1	1 0 1	0 1 0
1 0 1	0 0 0	0 1 0	1 0 1
1 0 1	1 1 1	1 0 1	1 0 1
1 0 1	0 0 0	0 1 0	0 1 0

A glide reflection is a translation accompanied

by a reflection across the axis of translation. In our case the glide is of length π , and our functions have period 2π . We require that our function be equivariant with respect to $\sigma(x,y)=(x+\pi,-y)$. If we attempt to equate the like terms in the equations resulting from the equivariance condition $g_A(\sigma(x,y)) = \sigma(g_A(x,y))$ we find the following.

$$a_{000} + a_{001}(-y) + a_{002}(-y)^2 + a_{100}\cos(x + \pi) + a_{101}(-y)\cos(x + \pi) + \dots = \\ \pi + a_{000} + a_{001}(y) + a_{002}(y)^2 + a_{100}\cos(x) + a_{101}(y)\cos(x) + \dots$$

and

$$a_{000} + a_{001}(-y) + a_{002}(-y)^2 + a_{100}\cos(x + \pi) + a_{101}(-y)\cos(x + \pi) + \dots = \\ -a_{000} - a_{001}(y) - a_{002}(y)^2 - a_{100}\cos(x) - a_{101}(y)\cos(x) + \dots$$

We find that equating constant terms requires that $\pi=0$, which is impossible, hence g_A is inadequate for the glide reflection. We create the family of functions $\left(\begin{matrix} x \\ 0 \end{matrix}\right) + g_A\left(\begin{matrix} x \\ y \end{matrix}\right) \bmod\left(\begin{matrix} 2\pi \\ \infty \end{matrix}\right)$ to deal with that difficulty. This addition of x to the first coordinate does not interfere with our translational equivariance as x modulo 2π is a periodic function. Requiring equivariance with respect to σ on our functions now

allows us to solve for the mask for this group. This mask, M_{p1a1} (see Table II), yields the family of functions $\begin{pmatrix} x \\ 0 \end{pmatrix} + g_{A^*M_{p1a1}} \begin{pmatrix} x \\ y \end{pmatrix} \bmod \begin{pmatrix} 2\pi \\ \infty \end{pmatrix}$. Figure 8 clearly shows a glide reflection. The parameters for this attractor and a compact implementation are given in the appendix.

We create the final two frieze patterns from combinations of the masks and function families we have already seen. The pma2 frieze pattern is characterized by lines of reflection perpendicular to the axis of translation, glide reflections, and two-fold rotations. The glide reflection requires we use $\begin{pmatrix} x \\ 0 \end{pmatrix} + g_A \begin{pmatrix} x \\ y \end{pmatrix} \bmod \begin{pmatrix} 2\pi \\ \infty \end{pmatrix}$. By combining the masks of pm11 and p1a1 we get a mask that will also generate the rotations, as well as require the desired symmetries for our function $\begin{pmatrix} x \\ 0 \end{pmatrix} + g_{A^*M_{pm11}^*M_{p1a1}} \begin{pmatrix} x \\ y \end{pmatrix} \bmod \begin{pmatrix} 2\pi \\ \infty \end{pmatrix}$. Figure 9 shows a chaotic attractor with these symmetries. Note the 180° rotation occurs at the midpoint between the lines of reflection.

The final frieze pattern, pmm2, contains reflections both parallel and perpendicular to the axis of translation, and a 180° rotation. This time the random array A is restricted by the combinations of M_{p1m1} and M_{pm11} and yields the function family $g_{A^*M_{p1m1}^*M_{pm11}} \begin{pmatrix} x \\ y \end{pmatrix}$. The resulting symmetries again generate the two-fold rotation. Figure 10 is an image representative of this group. Note the rotations fall on the intersections of lines of reflection as opposed to in between them.

4. CRYSTALLOGRAPHIC GROUPS

The crystallographic groups, or wallpaper groups, are characterized by translations in two independent directions, which give rise to a lattice. While frieze groups can contain only a two-fold rotation, the wallpaper groups may contain rotations of order two, three, four, and six. These different possible orders of rotation, along with independent translations, reflections, and glide reflections, yield a total of 17 possible crystallographic groups.

The simplest of the crystallographic groups is p1, which is characterized by two independent translations and no other symmetry. We find it convenient to use a function that is periodic in both the x and y directions. We choose a period of 2π in both directions, and the square determined by the perpendicular translation vectors is our generating region for p1. We recognize that using a square lattice does not impose additional symmetries on our

image as our chaotic attractors have no inherent symmetry. Note that we will use the square lattice as our fundamental region except for groups which use the hexagonal lattice.

It is known that smooth functions periodic in both x and y can be represented using a two-variable fourier series [21]. Thus we use a truncated double fourier series in both x and y to guarantee that our function is periodic in the x and y directions with period 2π . We truncate our fourier expansion at $2x$ and $2y$. Thus we get a function of the form:

$$h_A \begin{pmatrix} x \\ y \end{pmatrix} = \langle 1, \cos(x), \cos(2x), \sin(x), \sin(2x) \rangle \bullet A \bullet \langle 1, \cos(y), \cos(2y), \sin(y), \sin(2y) \rangle \bmod \begin{pmatrix} 2\pi \\ 2\pi \end{pmatrix}$$

where A is a 5 by 2 by 5 coefficient array. A coefficient of this array, a_{ijk} , is such that i represents the index of the fourier terms in x , j indicates the output coordinate, and k indicates the index in the fourier terms of y . Note that the result is mod 2π in both the x and y coordinates.

It is straightforward to check that this function is equivariant with respect to $\sigma_1(x,y)=(x+2\pi,y)$, and $\sigma_2(x,y)=(x,y+2\pi)$. Monte-Carlo searches were performed to create attractors for this group. Note that Figure 11 has only translational symmetry.

Once we have a function that is equivariant with respect to the two translations, combining masks allows us to create functions equivariant with respect to several crystallographic groups. The crystallographic group $p2$ introduces two-fold rotations. For our function to have the desired rotational symmetry, we require that it be equivariant with respect to $\sigma(x,y)=(-x,-y)$, as we did with a two-fold rotation in the $p112$ frieze group. The equivariance requires that $h_A(\sigma(x,y)) = \sigma(h_A(x,y))$. This implies:

$$\langle 1, \cos(-x), \cos(-2x), \sin(-x), \sin(-2x) \rangle \bullet A \bullet \langle 1, \cos(-y), \cos(-2y), \sin(-y), \sin(-2y) \rangle = \\ - (\langle 1, \cos(x), \cos(2x), \sin(x), \sin(2x) \rangle \bullet A \bullet \langle 1, \cos(y), \cos(2y), \sin(y), \sin(2y) \rangle).$$

Note that there are once again two separate equations, corresponding to the two coordinates of the maps. The above implies

$$a_{000} + a_{001} \cos(-y) + a_{002} \cos(-2y) + a_{003} \sin(-y) + a_{004} \sin(-2y) + \dots = \\ - a_{000} - a_{001} \cos(y) - a_{002} \cos(2y) - a_{003} \sin(y) - a_{004} \sin(2y) - \dots$$

and

$$a_{010} + a_{011} \cos(-y) + a_{012} \cos(-2y) + a_{013} \sin(-y) + a_{014} \sin(-2y) + \dots = \\ - a_{010} - a_{011} \cos(y) - a_{012} \cos(2y) - a_{013} \sin(y) - a_{014} \sin(2y) - \dots$$

Simplifying and equating like terms yields the array mask for p2 shown in Table III. Now we can write the family of functions for p2 as $h_{A^*M_{p2}}\begin{pmatrix} x \\ y \end{pmatrix}$. Figure 12 is an image resulting from Monte-Carlo searches for attractors across the parameter space.

The symmetry group pm is the most basic crystallographic group which contains reflections. The lines of reflection are placed such that the axes of reflection are parallel to one axis of translation and perpendicular to the other axis of translation, creating a rectangular lattice in the most general case. To generate a function with the pm symmetry, we require

equivariance with respect to $\sigma(x, y) = (x, -y)$. Note that this creates a mirror parallel to the horizontal translation vector; it could easily have been parallel to the vertical translation vector. The properties of equivariance imply certain coefficients must be zero, resulting in the mask for pm shown in Table III. It follows that the family of functions for pm has the form $h_{A^*M_{pm}}\begin{pmatrix} x \\ y \end{pmatrix}$. Figure 13, which illustrates such an attractor, has regions of high iteration falling near the line of reflection.

The most basic crystallographic group with glide reflections is pg. As with the glide reflection used for the frieze groups, we require that our function be equivariant with respect to $\sigma(x, y) = (x + \pi, -y)$. Note once again that the choice of a horizontal or vertical glide reflection axis is arbitrary. If we attempt to equate the terms in h required to be equal by equivariance, as for p1a1, π gets equated with zero. To avoid this contradiction, we use a new family of functions as before: $\begin{pmatrix} x \\ 0 \end{pmatrix} + h_A\begin{pmatrix} x \\ y \end{pmatrix} \bmod \begin{pmatrix} 2\pi \\ 2\pi \end{pmatrix}$. To reiterate, the addition of x to the first coordinate does not interfere with translational equivariance because x modulo 2π is a periodic function. Using the new family of functions, we find a mask to obtain equivariance with respect to a glide reflection of length π in the x direction.

Table III Array Masks for p2, pm, and pg.

p2	pm	pg
0 0 0 1 1	1 1 1 0 0	1 1 1 0 0
0 0 0 1 1	0 0 0 1 1	0 0 0 1 1
0 0 0 1 1	1 1 1 0 0	0 0 0 1 1
0 0 0 1 1	0 0 0 1 1	1 1 1 0 0
0 0 0 1 1	1 1 1 0 0	1 1 1 0 0
0 0 0 1 1	0 0 0 1 1	0 0 0 1 1
1 1 1 0 0	1 1 1 0 0	0 0 0 1 1
1 1 1 0 0	0 0 0 1 1	1 1 1 0 0
1 1 1 0 0	1 1 1 0 0	1 1 1 0 0
1 1 1 0 0	0 0 0 1 1	0 0 0 1 1

Figure 14 resulted from functions that had the form $\begin{pmatrix} x \\ 0 \end{pmatrix} + h_A * M_{pg} \begin{pmatrix} x \\ y \end{pmatrix} \bmod \begin{pmatrix} 2\pi \\ 2\pi \end{pmatrix}$.

Table IV
Array mask for
cm.

1 0 1 0 0
0 0 0 0 1
0 1 0 0 0
0 0 0 1 0
1 0 1 0 0
0 0 0 0 1
0 1 0 0 0
0 0 0 1 0
1 0 1 0 0
0 0 0 0 1

The symmetry group cm contains both reflections and glide reflections in parallel directions but no rotations. So, in addition to requiring equivariance with respect to translations, we require equivariance with respect to the symmetries $\sigma_1(x, y) = (x, -y)$ and $\sigma_2(x, y) = (x + \pi, \pi - y)$. Notice that for σ_1 the reflection is across the x-axis, and for σ_2 the glide reflection is across the line $y = \pi$. We need the extra term $\begin{pmatrix} x \\ y \end{pmatrix}$ instead of the $\begin{pmatrix} x \\ 0 \end{pmatrix}$ we used for pg since both coordinates of σ_2 include the constant π . Requiring equivariance with respect to σ_1 and σ_2 and equating like terms creates the function mask shown in Table IV. The family of functions for cm takes the form $\begin{pmatrix} x \\ y \end{pmatrix} + h_A * M_{cm} \begin{pmatrix} x \\ y \end{pmatrix} \bmod \begin{pmatrix} 2\pi \\ 2\pi \end{pmatrix}$. Note that $M_{cm} = M_{pm} * M_{g_{y=\pi}}$, where $M_{g_{y=\pi}}$ denotes the mask created by imposing equivariance with respect to the glide reflection along the line $y = \pi$. Figure 15 illustrates a chaotic attractor with this symmetry. The parameters for this image appear in the appendix.

The symmetry group pmm, which has perpendicular reflections, can make use of the existing mask used for pm to create a function that is equivariant with respect to the desired symmetries. In addition to being equivariant to translations, pmm must be equivariant with respect to $\sigma_1(x, y) = (x, -y)$ and $\sigma_2(x, y) = (-x, y)$. Since the mask for pm forces equivariance with respect to σ_1 , or horizontal reflections, we need only to design a mask which imposes equivariance with respect to σ_2 . It is not surprising that the resulting masks are related: for every $a_{ijk} = 0$ in the pm mask, the $a_{k(1-j)i}$ entry in the vertical reflection mask is also equal to zero. Combining the two masks via component-wise array multiplication, we obtain the pmm mask in shown in Table V. The functions with pmm symmetry then take on the form $h_A * M_{pmm} \begin{pmatrix} x \\ y \end{pmatrix}$. See Figure 16, and note the perpendicular axes of reflection with the absence of rotational symmetry.

The symmetry group pmg contains lines of reflection perpendicular to lines of glide reflection. The family of functions takes on the form $\begin{pmatrix} 0 \\ y \end{pmatrix} + h_A * M_{pmm} * M_{g_{x=0}} \begin{pmatrix} x \\ y \end{pmatrix} \bmod \begin{pmatrix} 2\pi \\ 2\pi \end{pmatrix}$, where $M_{g_{x=0}}$ is the function mask derived by requiring the function be equivariant with respect to a glide reflection of length π along the line $x=0$. Figure 17 is an example of an attractor with pmg symmetry; note the two distinct glide reflections.

The wallpaper group pgg has perpendicular glide reflections. The family of functions takes on the form $\begin{pmatrix} x \\ y \end{pmatrix} + h_A * M_{pgg} \begin{pmatrix} x \\ y \end{pmatrix} \bmod \begin{pmatrix} 2\pi \\ 2\pi \end{pmatrix}$, because there

are now glide reflections in both the x and y directions. Note that in Figure 18 two-fold rotations appear, resulting from perpendicular glide reflections.

The group cmm is similar to pmm in that it contains perpendicular reflection axes, but it also contains rotations of order two which do not lie on the reflection axes. Glide reflections also exist, resulting from combining perpendicular mirrors and half turns, so our function should be equivariant with respect to four symmetries: $\sigma_1(x,y) = (x,-y)$, $\sigma_2(x,y) = (-x,y)$, $\sigma_3(x,y) = (x+\pi,\pi-y)$, and $\sigma_4(x,y) = (\pi-x,y+\pi)$. The family of functions takes the form $\begin{pmatrix} x \\ y \end{pmatrix} + h_A * M_{cmm} \begin{pmatrix} x \\ y \end{pmatrix} \bmod \begin{pmatrix} 2\pi \\ 2\pi \end{pmatrix}$. The mask M_{cmm} is the product $M_{pmm} * M_{g_{y=\pi}} * M_{g_{x=\pi}}$. Note that in Figure 19, the intersection of perpendicular glide reflections occurs a half-period away in both directions from the intersection of the perpendicular mirror reflections.

The most general symmetry group that contains a four-fold rotation is p4. For a function to have this symmetry, we require it be equivariant to $\sigma(x,y)=(-y,x)$. The implications of placing this requirement on h_A are as follows:

Table V Array masks for pmm, pmg, pgg.

pmm	pmg	pgg
00000	01000	01000
00011	00001	00001
00000	01000	00010
00011	00001	10100
00000	01000	01000
00011	00001	00001
11100	10100	00001
00000	00010	01000
11100	10100	10100
00000	00010	00010

Table VI
Array mask for cmm

00000
00001
00000
00010
00000
00001
01000
00000
10100
00000

$$a_{000}=a_{010}, a_{001}=a_{110}, a_{002}=a_{210}, \dots$$

$$\dots, a_{300}=-a_{013}, a_{301}=-a_{113}, a_{302}=-a_{213}, \dots$$

More specifically stated, $a_{i0k}=a_{k1i}$ for the first three planes of A (where $0 \leq i \leq 2$ and $0 \leq k \leq 4$) and $a_{i0k}=-a_{k1i}$ for the last two planes of A (where $3 \leq i \leq 4$ and $0 \leq k \leq 4$). The irregular pattern of minus signs and indices here is caused jointly by the swapping of x and y by σ and the even and odd nature of our trigonometric functions.

Thus we find it useful to define the function $T : M_{525}(\mathfrak{R}) \rightarrow M_{525}(\mathfrak{R})$ by $T(A)=B$, where $b_{i0k}=a_{i0k}$, $b_{i1k}=a_{k0i}$ for $0 \leq i \leq 2$ and $0 \leq k \leq 4$, and $b_{i1k}=-a_{k0i}$ for $3 \leq i \leq 4$ and $0 \leq k \leq 4$. So T converts an array A to the form we desire. Hence we use $h_{T(A)}$ as our function for generating attractors that fit the symmetry group $p4$. The example in Figure 20 displays centers of four-fold rotation in the centers of each empty region and each colored region, as well as centers of two-fold rotation on the connections between the masses.

The symmetry group $p4m$ contains the four-fold rotational symmetry of group $p4$ as well as perpendicular lines of reflection. We used the function from group $p4$ coupled with the mask of the group pm , obtaining $h_{T(A)*M_{pm}}$ which is equivariant with respect to $p4m$. We only need apply the mask corresponding to $\sigma_{(x,y)}=(x,-y)$, representative of one horizontal line of reflection, for coupling this with the four-fold rotational symmetry creates perpendicular lines of reflection. In this manner we obtain images such as Figure 21, in which one can spot centers of four-fold and two-fold rotation, in addition to horizontal and vertical lines of reflections through the centers of four-fold rotation.

Using a similar tactic to our extension of $p4$ to $p4m$, we extend $p4$ to $p4g$. As with previous groups involving glide reflections, we add a special term; here we add the vector $\begin{pmatrix} x \\ y \end{pmatrix}$ and reduce modulo 2π in both coordinates to fulfill our equivariance condition.

Hence the function $\begin{pmatrix} x \\ y \end{pmatrix} + h_{T(A)*M_{pg}} \begin{pmatrix} x \\ y \end{pmatrix} \pmod{\begin{pmatrix} 2\pi \\ 2\pi \end{pmatrix}}$ generates $p4g$ images such as the one in Figure 22. Lines of glide reflection pass horizontally and vertically through the centers of four-fold rotation.

The symmetry group $p3$ has third turns in addition to two independent translations. Since a square lattice does not map to itself by third turns, we need to use a different lattice. Indeed, a lattice with 120° angles between the independent directions is appropriate. We take $u_0 = 2\pi(1,0)$ and $u_1 = 2\pi(-1/2, \sqrt{3}/2)$ as the generators of our lattice L . Connecting vertices in this lattice yields a regular tiling of the plane by equilateral triangles and blocks of six give hexagons; hence this is called a hexagonal lattice. The

vectors $v_0 = (1, -1/\sqrt{3})$ and $v_1 = (0, -2/\sqrt{3})$ form a basis for the dual lattice L^* . In particular, for all i and j , $u_i \bullet v_j$ is an integer multiple of 2π . Thus, if u denotes any element of L and v is any element of L^* then $u \bullet v$ is an integer multiple of 2π and hence $\cos(v \bullet (X + u)) = \cos(v \bullet X)$ and $\sin(v \bullet (X + u)) = \sin(v \bullet X)$. Consider the function $F : \mathfrak{R}^2 \rightarrow \mathfrak{R}^2$ defined by

$$F(X) = \sum_{v \in V} (\alpha_v \cos(v \bullet X) + \beta_v \sin(v \bullet X)) \text{ mod } L$$

where V is a finite subset of the dual lattice L^* and $\alpha_v, \beta_v \in \mathfrak{R}^2$ are constant vectors. If σ is any translational symmetry of L then the above remarks help us verify that $F(X)$ is equivariant with respect to σ . Now if we also want to require that our maps are equivariant with respect to third turns about the origin we can insist that whenever one term appears, so do two others. Let $M = \begin{pmatrix} -1/2 & -\sqrt{3}/2 \\ \sqrt{3}/2 & -1/2 \end{pmatrix}$, then $R(X) = M X$

designates a counterclockwise rotation by 120° . Now if v is in the dual lattice and $\alpha_v \in \mathfrak{R}^2$ then

$$G_v(X) = \alpha_v \cos(v \bullet X) + R(\alpha_v) \cos(R(v) \bullet X) + R^2(\alpha_v) \cos(R^2(v) \bullet X) \text{ mod } L$$

is equivariant with respect to the translations from the original lattice L and we can see it is also equivariant with respect to R as follows:

$$R(G_v(X)) = R(\alpha) \cos(v \bullet X) + R^2(\alpha) \cos(R(v) \bullet X) + \alpha \cos(R^2(v) \bullet X) \text{ while}$$

$$G_v(R(X)) = \alpha \cos(v \bullet R(X)) + R(\alpha) \cos(R(v) \bullet R(X)) + R^2(\alpha) \cos(R^2(v) \bullet R(X)).$$

The facts that $v \bullet R(X) = R^2(v) \bullet X$, $R(v) \bullet R(X) = v \bullet X$, and $R^2(v) \bullet R(X) = R(v) \bullet X$ follow from the matrix form for R and these give $G_v(R(X)) = R(G_v(X))$ which is the desired equivariance. An analogous sum of sine terms,

$$H_v(X) = \beta_v \sin(v \bullet X) + R(\beta_v) \sin(R(v) \bullet X) + R^2(\beta_v) \sin(R^2(v) \bullet X) \text{ mod } L,$$

also has these equivariance properties.

We define a family of functions used to create attractors with p3 symmetry based on a random 2 by 3 by 2 array A of parameters as follows. We take our finite set in the dual lattice to be $V = \{v_0, v_1, v_2\}$ where v_0 and v_1 were specified above and $v_2 = v_0 + v_1$. We consider functions of the form

$$\sum_{j=0}^2 G_{v_j}(X) + H_{v_j}(X) \text{ mod } L$$

where $\alpha_{v_j} = \begin{pmatrix} a_{0j0} \\ a_{0jl} \end{pmatrix}$ and $\beta_{v_j} = \begin{pmatrix} a_{1j0} \\ a_{1jl} \end{pmatrix}$. Thus, the indices of the coefficients a_{ijk} are

ordered so that i selects cosine or sine, j corresponds to the elements in V , and k

corresponds to the fact that the coefficients are chosen from \mathfrak{H}^2 and hence have two coordinates. Figure 23 shows an example of an attractor with these three-fold rotations generated by this type of function. Notice that there are two independent nonorthogonal translations and that there are three different types of threefold rotations.

The symmetry group p3m1 has the symmetries of p3 with the addition of mirrors going through each 3-fold rotation. This can be accomplished by adding a mirror along the y axis in our model for p3. Namely, we require equivariance with respect to $\sigma_y(x, y) = (-x, y)$. Now the terms of $G_v(\sigma_y(x, y))$ and $\sigma_y(G_v(x, y))$ are not the same. Nonetheless, the terms of $G_v(\sigma_y(x, y))$ are nearly the same as those from $G_{\sigma_y(v)}(x, y)$ since $v \bullet \sigma_y(X) = \sigma_y(v) \bullet X$; however, the coefficients are not quite correct. We add together two terms of the form $G_v(X)$ with related constants to get a new function with the desired equivariance. Let

$$\hat{G}_{v, \sigma_y}(X) = G_v(X) + G_{\sigma_y(v)}(X) \text{ mod } L$$

where the constants for the second term are chosen so that $\alpha_{\sigma_y(v)} = \sigma_y(\alpha_v)$. Namely,

$$\begin{aligned} \hat{G}_{v, \sigma_y}(X) = & \alpha_v \cos(v \bullet X) + R(\alpha_v) \cos(R(v) \bullet X) + R^2(\alpha_v) \cos(R^2(v) \bullet X) \\ & + \sigma_y(\alpha_v) \cos(\sigma_y(v) \bullet X) + R(\sigma_y(\alpha_v)) \cos(R(\sigma_y(v)) \bullet X) + R^2(\sigma_y(\alpha_v)) \cos(R^2(\sigma_y(v)) \bullet X) \text{ mod } L. \end{aligned}$$

Now we know $\hat{G}_{v, \sigma_y}(X)$ is equivariant with respect to the translations and third turns

since it is the sum of such functions and we can check directly that it is equivariant with respect to σ_y ; however this requires using facts noted above along with relations between R and σ_y such as $R \sigma_y = \sigma_y R^2$. We note that we can construct another class of equivariant functions, which we will denote $\hat{H}_{v, \sigma_y}(X)$, using sines instead of cosines

and β_v as the coefficients. Then taking the sum $\sum_{j=0}^2 \hat{G}_{v_j, \sigma_y}(X) + \hat{H}_{v_j, \sigma_y}(X) \text{ mod } L$ gives

a family of functions whose parameters can be given by a 2 by 3 by 2 array as was the case for the p3 symmetry group. Figure 24 shows an example of an attractor constructed by such a function. Notice the variety of triangles, near circular patterns and that the three different third turns all lie on mirrors as required. The parameters and sample code for generating this image are given in the appendix.

The symmetry group p31m again has third turns and mirrors in addition to translational symmetry. However, only one of the types of third turns lies on a mirror in this group. In our model we can require equivariance with respect to a reflection across the x-axis; that is, with respect to $\sigma_x(x, y) = (x, -y)$. Consider the functions

$$\sum_{j=0}^2 \hat{G}_{v_j, \sigma_x}(X) + \hat{H}_{v_j, \sigma_x}(X) \text{ mod } L \text{ where the convention now requires } \alpha_{\sigma_x(v)} = \sigma_x(\alpha_v)$$

and likewise for the $\beta_{\sigma_x(v)} = \sigma_x(\beta_v)$ coefficients. We see these functions are equivariant with respect to the translations, the third turns and σ_x in the same manner as the analysis for p3m1. However, the symmetry group is subtly different; two of the three different types of third turns do not lie on mirrors. In Figure 25 we see that there are obvious third turns on mirrors and light third turn pinwheels.

The symmetry group p6 is generated by two independent translations and a sixth turn. Again we use a hexagonal lattice about the origin. If we let $N = \begin{pmatrix} 1/2 & -\sqrt{3}/2 \\ \sqrt{3}/2 & 1/2 \end{pmatrix}$, then $S(X) = NX$ designates a counterclockwise rotation by 60° . Redefine $G_v(X)$ in this situation as follows.

$$G_v(X) = \sum_{j=0}^5 S^j(\alpha_v) \cos(S^j(v) \bullet X) \text{ mod } L$$

We can check this is equivariant with respect to the translations and S ; we can take advantage of the fact that $S^j(v) \bullet S(X) = S^{j-1}(v) \bullet X$. Likewise

$$H_v(X) = \sum_{j=0}^5 S^j(\beta_v) \sin(S^j(v) \bullet X) \text{ mod } L$$

is equivariant with respect to the translations and S . Hence we can use the function family

$$\sum_{j=0}^2 G_{v_j}(X) + H_{v_j}(X) \text{ mod } L$$

to produce attractors with the desired symmetry. Note our parameters again can be arranged in a 2 by 3 by 2 array A where the indices of a_{ijk} are ordered so that i selects cosine or sine, j corresponds to the elements in V , and k corresponds to the fact that the coefficients are chosen from \mathfrak{R}^2 . Figure 26 shows an example of an attractor with these six-fold rotations and the two independent translations. Notice that there are numerous other symmetries forced by those symmetries: half-turns and third turns, for example.

The last crystallographic symmetry group is p6m which has the symmetries of p6 along with a mirror through the sixth turns. It turns out we can obtain this group by putting a mirror along either axis and we choose equivariance with respect to $\sigma_x(x, y) = (x, -y)$.

Consider

$$\hat{G}_{v, \sigma_x}(X) = G_v(X) + G_{\sigma_x(v)}(X) \text{ mod } L$$

where we use the S form for the G_v functions and the constants for the second term are again chosen so that $\alpha_{\sigma_x(v)} = \sigma_x(\alpha_v)$. As was the case for p31m, we can check that those functions are equivariant with respect to the translations, S and σ_x . Similar statements can be made for

$$\hat{H}_{v,\sigma_x}(X) = H_v(X) + H_{\sigma_x(v)}(X) \bmod L$$

which uses sines and β_v instead of cosines and α_v . Then taking the sum $\sum_{j=0}^2 \hat{G}_{v_j,\sigma_x}(X) + \hat{H}_{v_j,\sigma_x}(X) \bmod L$ gives a family of functions whose parameters can be given by a 2 by 3 by 2 array A as in our other hexagonal lattice families. These functions have the desired equivariance properties. Figure 27 shows an example of an attractor that has p6m symmetry. Notice the sixth turns lie on lines of reflection and additional symmetries include third turns.

5. CONCLUSIONS

One can create chaotic attractors that are forced to have any of the discrete symmetry groups of the plane. This is accomplished by the construction of suitable families of functions equivariant with respect to each symmetry group followed by Monte Carlo searches through parameter space. The frieze groups take advantage of fourier series in one direction and a power series in the other. In most cases additional symmetry can be added by masking the parameter space. Glide reflections require special consideration; addition of a special term allows us to construct families with finitely many terms that have equivariance with regard to those symmetries. Most of the crystallographic groups are implemented using double fourier series. Again, many of the symmetries can be obtained using a mask of the parameter space, but special terms are required for glide reflections, and quarter turns introduce conditions on the parameter space more complex than a mask. Symmetry groups that contain third or sixth turns require a hexagonal lattice. Here our families of equivariant functions make use of a dual lattice, and rotational and reflective symmetry is added by summing suitable terms. Images of these attractors often have a striking appearance when the Ljapunov exponent is positive and this allows for the construction of beautiful examples.

Acknowledgements – This research was supported in part by NSF grant DMS-9424098 and Lafayette College.

REFERENCES

- [1] E. N. Lorenz, Deterministic nonperiodic flow, *Journal of Atmospheric Science*, **20**, 13-141 (1963).
- [2] I. Stewart and M. Golubitsky, *Fearful Symmetry*, Blackwell Publishers, Oxford (1992).

- [3] M. Zhu and J. D. Murray, Parameter Domains for Spots and Stripes in Mechanical Models for Biological Pattern Formation, *Journal of Nonlinear Science*, **5** 4, 317-336 (1995).
- [4] G. M. Zaslavsky, R. Z. Sagdeev, D. A. Usikov, A.A. Chernikov, *Weak Chaos and Quasi-regular Patterns*, Cambridge University Press, Cambridge, (1991).
- [5] D. Schattschneider, *Visions of Symmetry: notebooks, Periodic Drawings and Related Work of M. C. Escher*, Freeman, New York (1990).
- [6] H. Weyl, *Symmetry*, Princeton University Press, Princeton, (1952).
- [7] D. W. Thompson, *On Growth and Form*, 2nd edition, Cambridge University Press, Cambridge (1963).
- [8] B. Grünbaum, G.C. Shephard. *Tilings and Patterns*. W.H. Freeman and Company, New York, (1989).
- [9] M. Field, M. Golubitsky. *Symmetry in Chaos*. Oxford University Press, New York, (1992).
- [10] M. Field, M. Golubitsky, Symmetric Chaos: how and why, *Notices of the AMS* **42**, 240-244 (1995).
- [11] G. Brisson, K. Gartz, B. McCune, K. O'Brien, C. Reiter. Symmetric Attractors in Three-dimensional Space. *Chaos, Solitons, and Fractals*, **7**, 1033-1051 (1996).
- [12] C. A. Reiter, Attractors with the Symmetry of the n -Cube, *Experimental Mathematics*, **5** 4, 327-336 (1996).
- [13] C. A. Reiter, Chaotic Attractors with the Symmetry of the Tetrahedron, *Computers & Graphics*, to appear.
- [14] J.C. Sprott, Automatic Generation of Strange Attractors, *Chaos and Graphics*, **17**, 325-332 (1993).
- [15] H.-O. Peitgen, H. Jürgens and D. Saupe, *Chaos and Fractals*, Springer-Verlag, New York (1992).
- [16] T. Parker, L. Chua, *Practical Numerical Algorithms for Chaotic Systems*. Springer-Verlag, New York (1989).
- [17] B. Goertzel, Rapid Generation of Strange Attractors with the Eugenic Genetic Algorithm, *Computers & Graphics*, **19** 1, 151-156, (1995).
- [18] P. Ashwin and I. Melbourne, Symmetry groups of attractors, *Archive for Rational Mechanics and Analysis* **126**, 59-78 (1994).
- [19] I. Melbourne, M. Dellnitz and M. Golubitsky, The structure of symmetric attractors, *Archive for Rational Mechanics and Analysis* **123**, 75-98 (1993).

- [20] C. A. Reiter, Attractors with Dueling Symmetry, *Computers & Graphics*, **21** 2, 263-271 (1997).
- [21] G. P. Tolstov, *Fourier Series*, Translated by R. A. Silverman, Prentice-Hall, Englewood Cliffs, NJ, (1962).
- [22] N. Carter, R. Eagles, S. Grimes, A. Hahn and C. Reiter, Chaos with Symmetry: reflections on an exhibition, to appear in the *Proceedings of APL97, CDROM*, Toronto, Ontario (1997).
- [23] C. Reiter, Creating Images in J, to appear in the *Proceedings of APL97, CDROM*, Toronto, Ontario, (1997).
- [24] K. E. Iverson, *J Introduction and Dictionary*, Iverson Software Inc., Toronto Ontario, (1995).
- [25] C. A. Reiter, *Fractals, Visualization and J*, Iverson Software, Inc., Toronto (1995).

Appendix

This appendix contains the parameter values and function definitions for Figures 8, 15 and 24. A few details of our implementation are given so that readers exploring the attractors in this paper should be able to verify their function implementations. Our examples were constructed using J which is not widely known but is available for downloading from www.jsoftware.com. Very preliminary versions of a couple of the constructions of attractors with planar symmetry given in this paper also appear in [22, 23]. Readers interested in creating their own attractors with symmetries as we have described will be interested in the parameter values and sample function values appearing below. Since little additional space was required to add enough J so readers can also create their own versions of these images, that is also done, though the meaning of the code is not transparent to the uninitiated. Readers creating high resolution versions of these images in J are encouraged to study the J documentation, [24] and/or [25].

```
x=:+/. *          matrix multiplication
sin=:1&o.
cos=:2&o.
min=:<./
max=:>./
floor=:<.
```

FZ2 creates functions with p1a1 symmetry from suitable parameters.

```
FZ2 =: 1 : '(2p1&|@{.,{:})@(({:.,0:)+(1: , 2&o. , 2&o.@+: ,
1&o., 1&o.@+:))@{. x m."_ x ^&(i.3)@{:}) f.'
```

```

par08=: 5 2 3$;<@".;. 2]0 : 0      parameters for Figure 8
0.831722      0  0.0138725
0      0.255773  0

0      0.137478      0
0.156811  0  0.0538264

0.659532      0  0.74701
0  0.715334  0

0      0.44344      0
_0.506331      0  0.461773

0.980024      0  0.649317
0      0.75199  0
)

```

```
f08=: par08t FZ2      function for Figure 8
```

WP2 creates functions with cm symmetry from suitable parameters.

```

WP2=: 1 : '2p1&|@(+({. x m."_ x {:})@:(1: ,. cos ,. cos@+: ,.
      sin ,. sin@+:)) f.'

```

```

par15=: 5 2 5$;<@".;. 2]0 : 0      parameters for Figure 15
0.0767508      0  0.804914      0      0
0      0      0      0  0.530214

0      0.265496      0      0      0
0  0.926566      0

0.967418      0  0.980258      0      0
0      0      0      0  0.563521

0      0.539515      0      0      0
0      0      0  0.10244      0

_0.549542      0  0.322755      0      0
0      0      0      0  0.704369
)

```

```
f15=:par15 WP2
```

WP3 creates functions with p3m1 symmetry from parameters.

```

WP3=: 1 : 0
fu2r=. (2p1, o. %:3) &|"1 NB. fund unit to rect
L=. (l1=.2p1 0), .l2=.2p1*(2 1 o. 2r3p1)
fup=. 1&| &. (%&L)
R=.x&(((cos, sin), :-@sin, cos) 2r3p1)

```

```

M=.R^(i.3)"2 m.
v=.R^(i.3)(1 0,0 1,:1 1)x(1,-%:3),:0,_2%:3
sig=.(1 1)&"1
fup@:(+/^:3)@:(M" _ *"1 0 ]>@:(cos,:sin)@:(v&x) + ((sig M)" _
      *"1 0 ]>@:(cos,:sin)@:(sig v)&x) f.
)

```

```

par24=: 2 3 2$;<@".;._2]0 : 0           parameters for Figure 24
_0.0966238 0.0436792
_0.116669 0.852935
_0.713108 0.796924

_0.0978695 _0.892281
_0.569655 _0.186624
_0.58311 _0.332584
)

```

```
f24=:par24 WP3
```

We next display iterates 10 to 14 on initial guess 0.1 0.2 for each of the functions created as a check for implementations.

```

f08^(10+i.5)0.1 0.2
2.55032 0.0824602
2.75651 0.473115
3.21827 0.0158882
4.84963 0.112226
4.84338 0.445774
f15^(10+i.5)0.1 0.2
1.62329 2.88606
1.78365 2.95051
2.085 3.03449
2.54699 3.07267
3.11211 3.0119
f24^(10+i.5)0.1 0.2
_0.40199 1.52887
_5.17233 1.34564
3.93791 0.853705
4.74573 2.32464
_0.399799 4.18074

```

Lastly, we offer a quick construction of a small version of Figure 8 for those who wish to explore these images in J. Explanations of the J details are skipped but the online help could be used fill in the meaning of primitives. This section assumes the reader has run the above definitions and the script raster3.js that comes with the J extras.

```
xy=.f08t^(1000+i.10000) 0.1 0.2 Get 10,000 iterates
```

```

min xy
0.00121 2.39929
max xy
6.28244 2.39933

```

Rescale to pixel coords:

```

XY =.floor (200 % 6.283 4.8)*"1 (0 2.4)+"1 xy
3{.XY                                     the first three lit pixels
196 196
121 73
176 90

n=.~.XY                                     pixels hit
fq=#/.~ XY                                 their frequency count
max fq
32
pal=.255,hue 5r6*(i.%<:) 32             palette with 32 colors

```

Insert frequencies in 200 by 200 zero matrix:

```

b=. |:fq (<"1 n)}200 200$0
(pal;b) writebmp8 'fig08.bmp'

```

The last command should create a low resolution, but color, windows bitmap with the attractor seen in Figure 8. One can use similar constructions to create Figures 15 and 24.

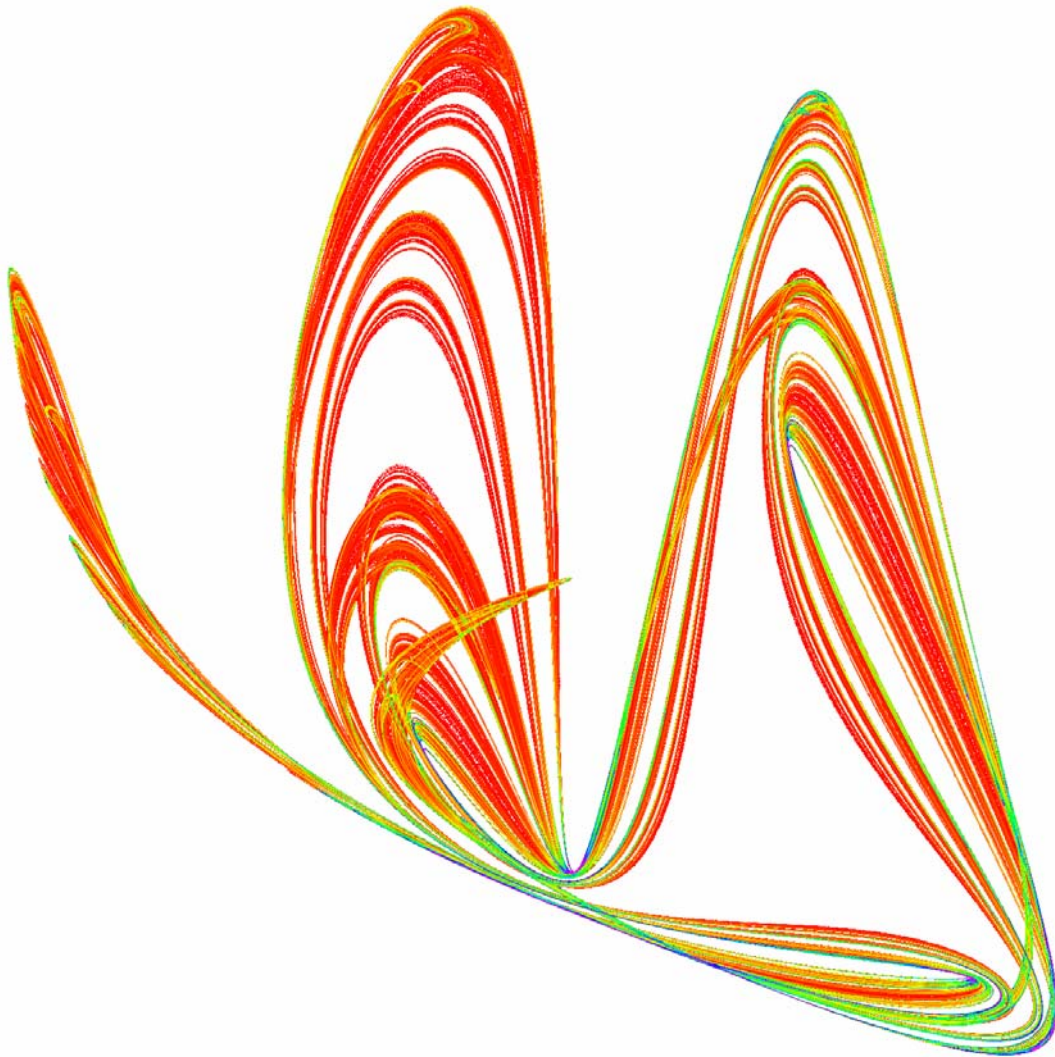


Figure 1. C1: A chaotic attractor in the plane with no symmetry.

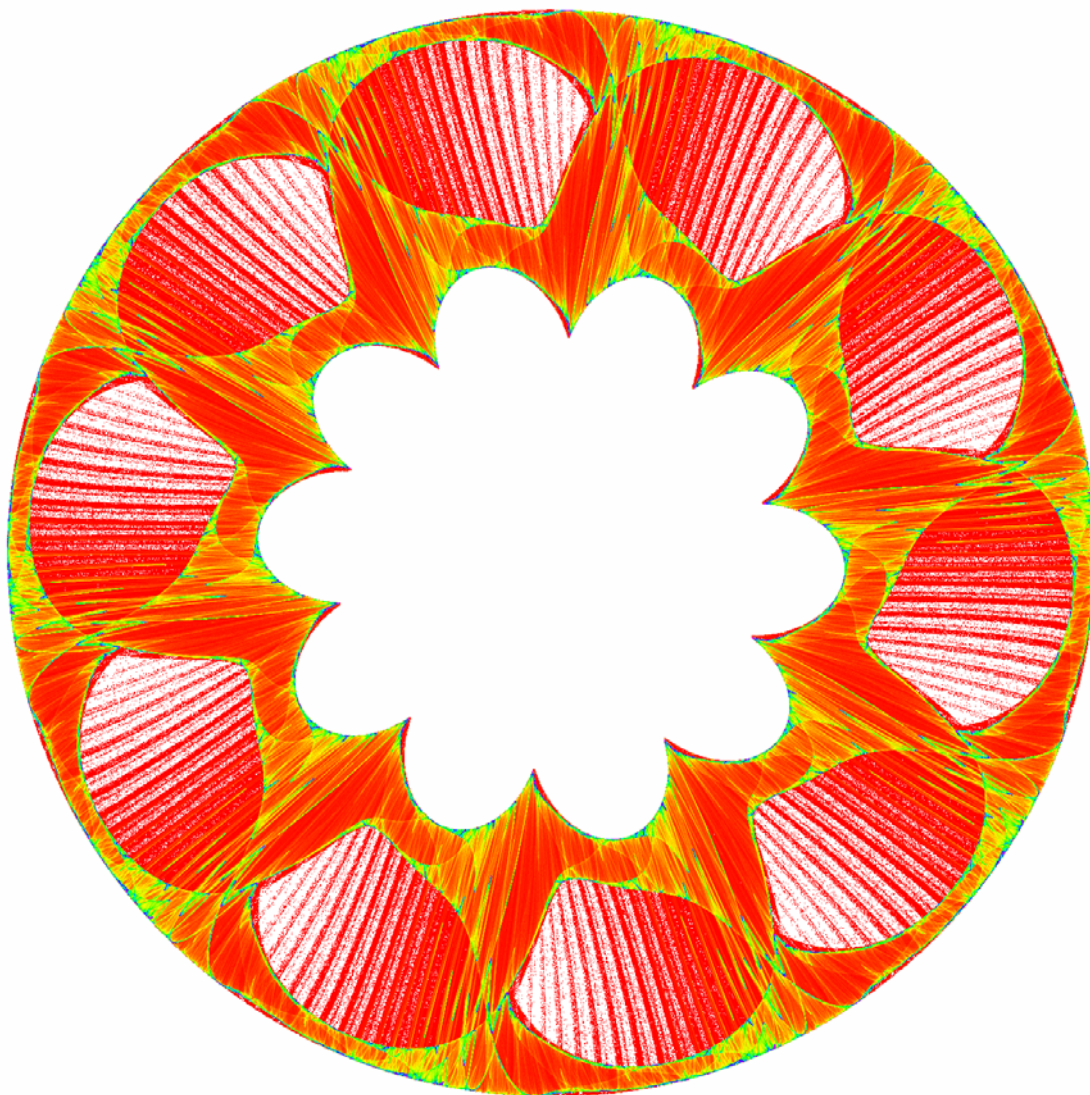


Figure 2. C10: An attractor with 10-fold cyclic symmetry.

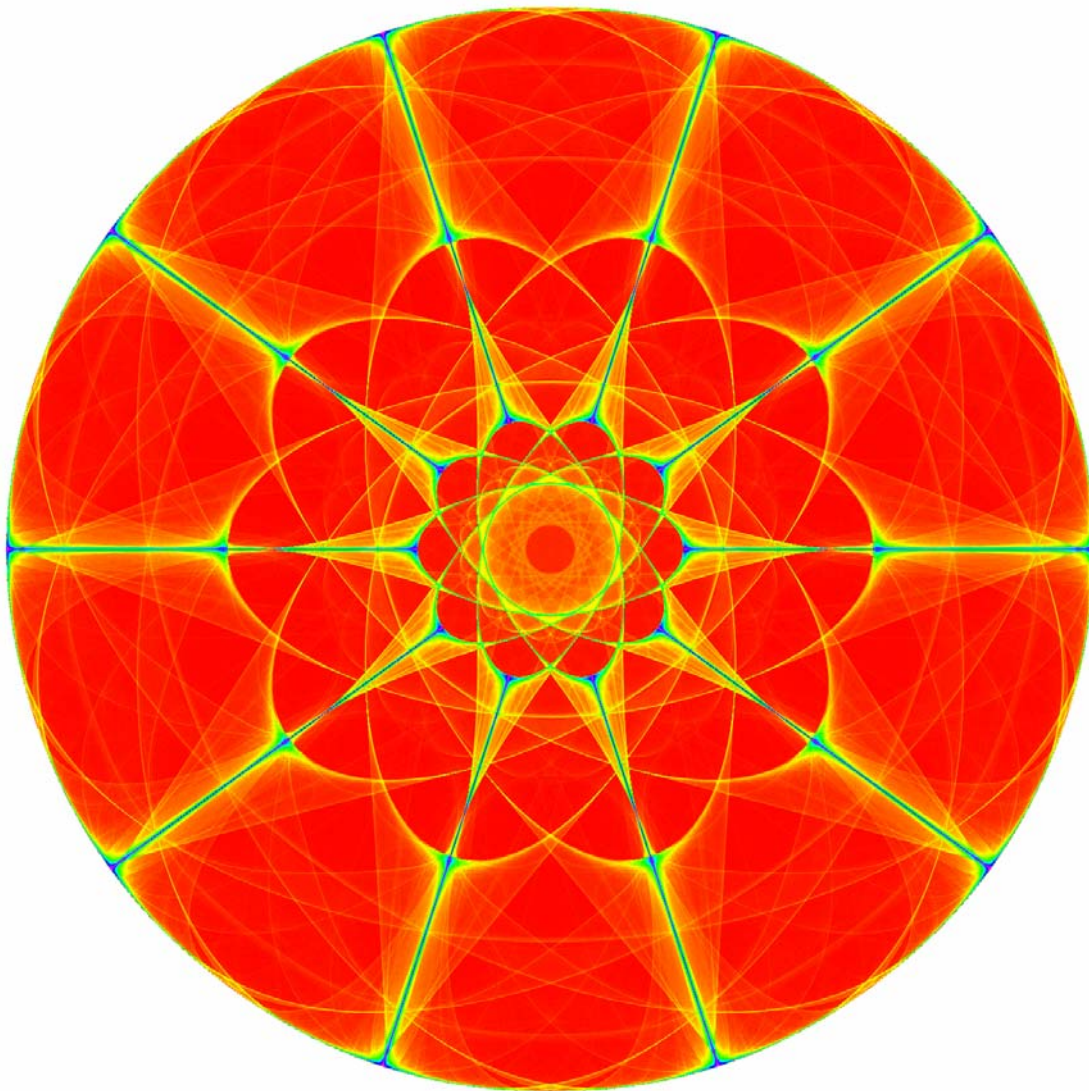


Figure 3. D10: An attractor with 10-fold dihedral symmetry.

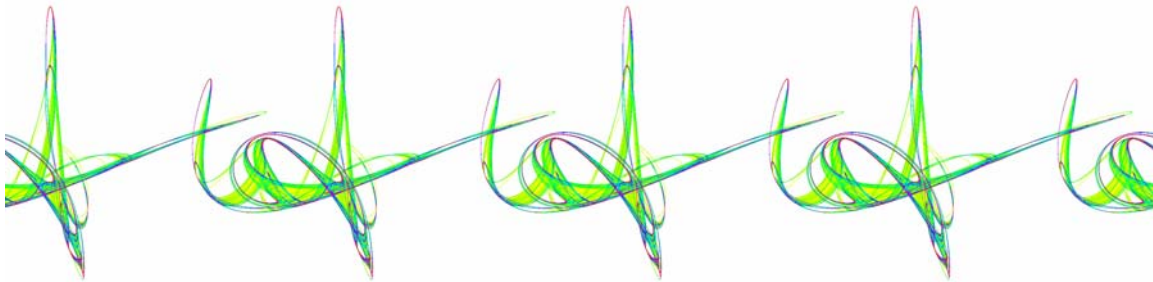


Figure 4. P111: An attractor with translational symmetry

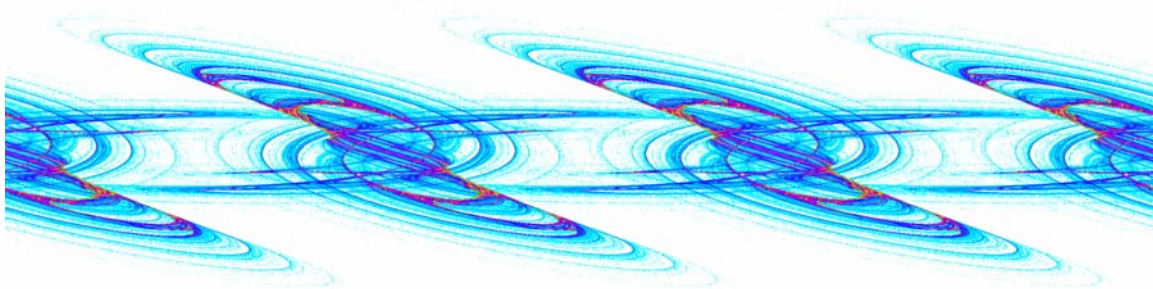


Figure 5. P112: An attractor with a translation and a half turn.

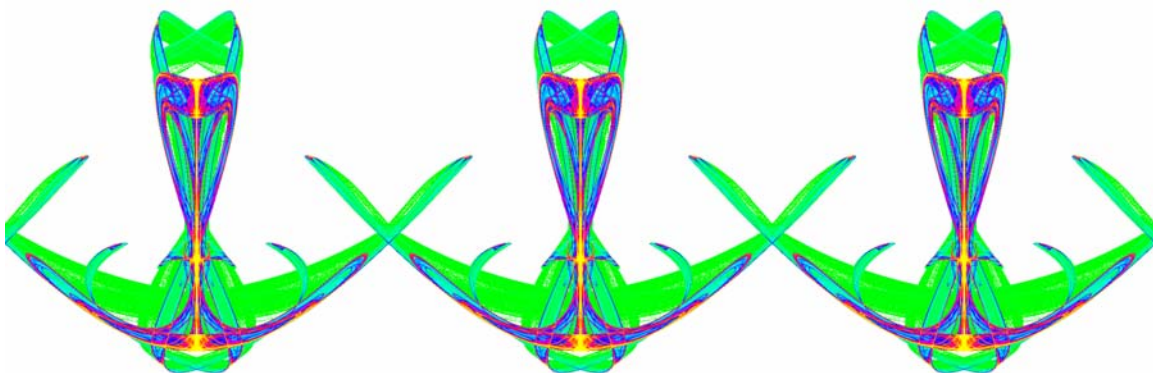


Figure 6. PM11: An attractor with a translation and a horizontal reflection.

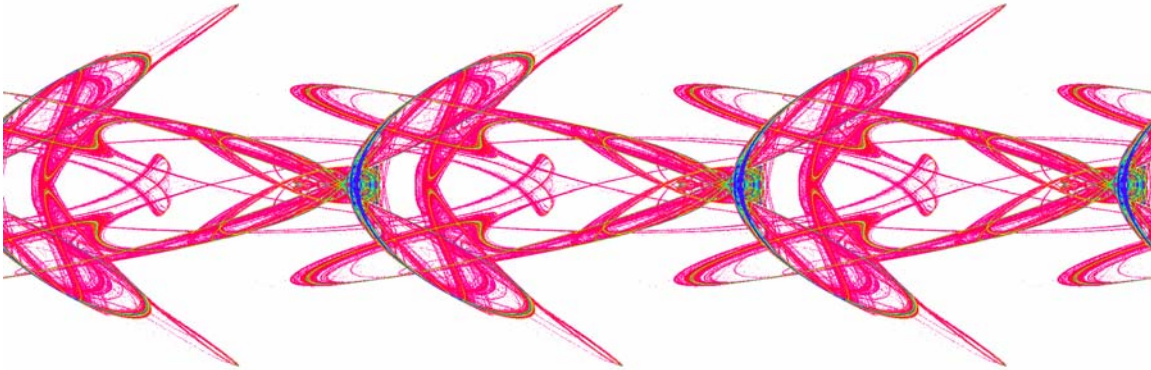


Figure 7. An attractor with a translation and vertical reflection.

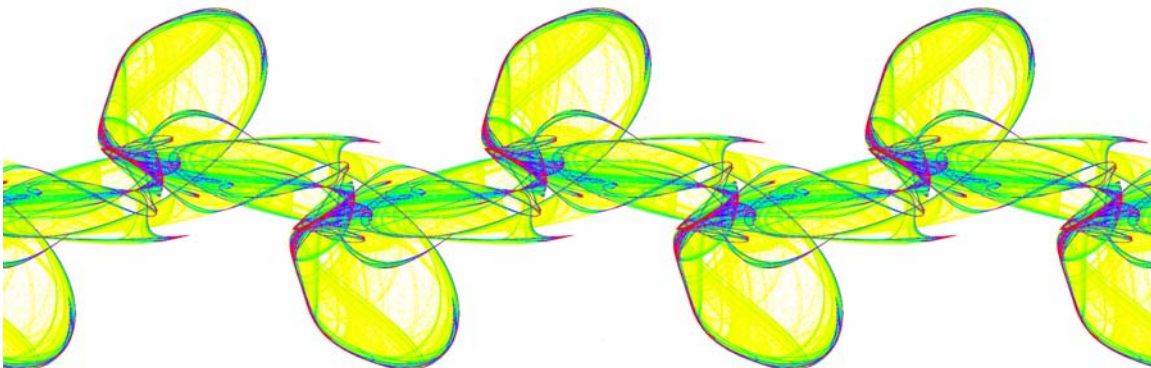


Figure 8. P1A1: An attractor with a translation and a glide reflection

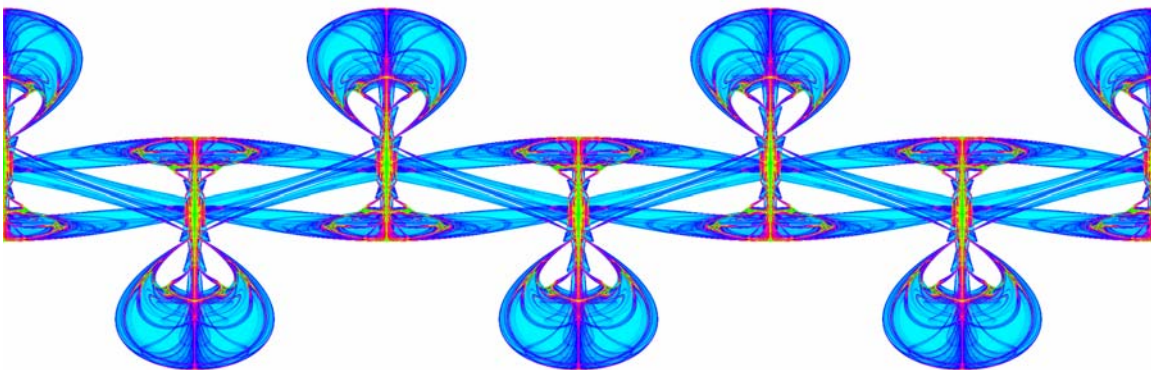


Figure 9. PMA2: An attractor with a translation and horizontal and vertical reflections.

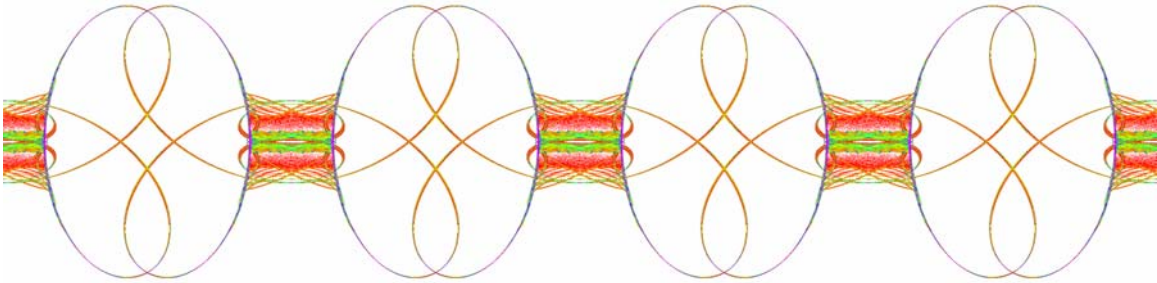


Figure 10: PMM2: An attractor with horizontal and vertical reflections.

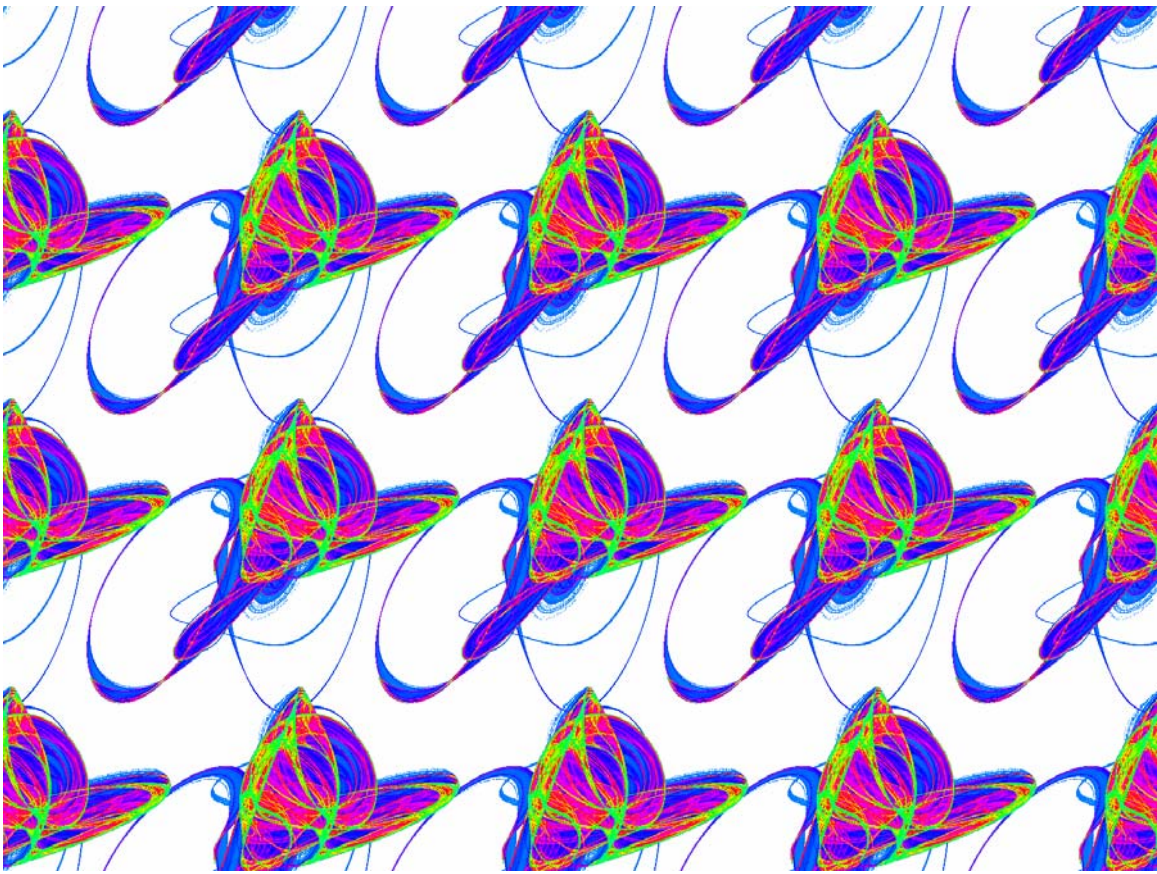


Figure 11: P1: An attractor with two translations.

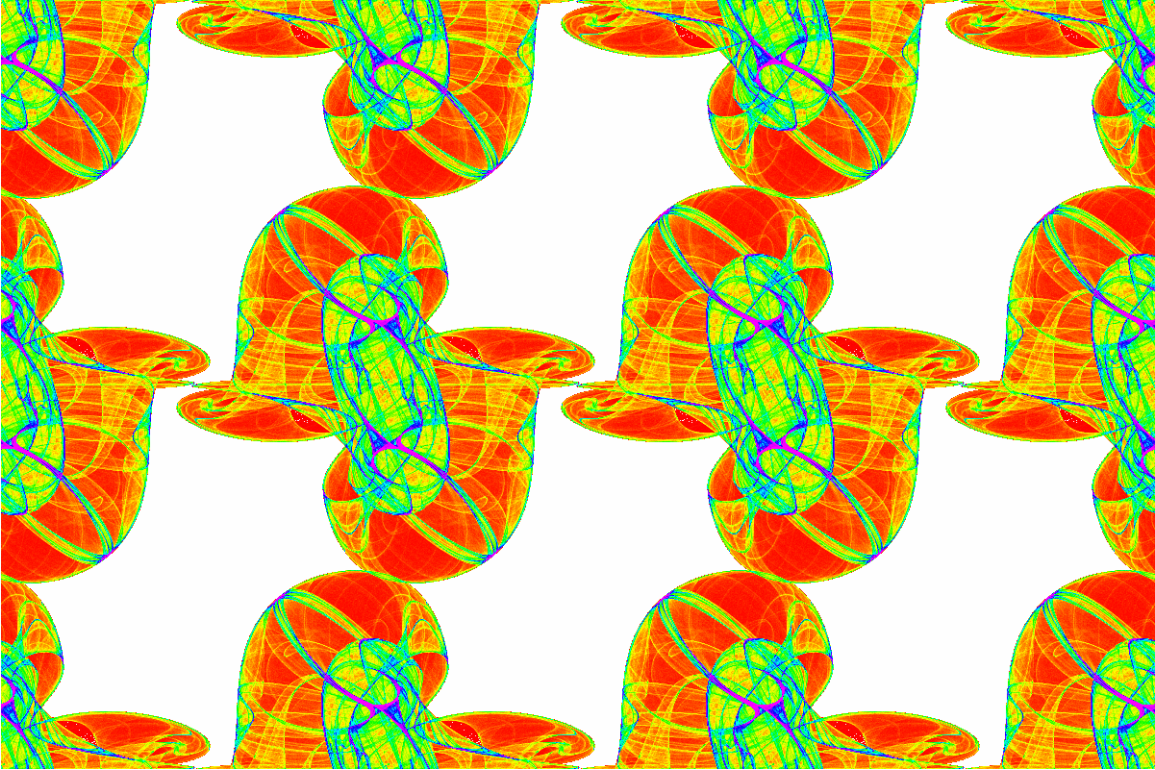


Figure 12: P2: An attractor with two translations and a half turn.

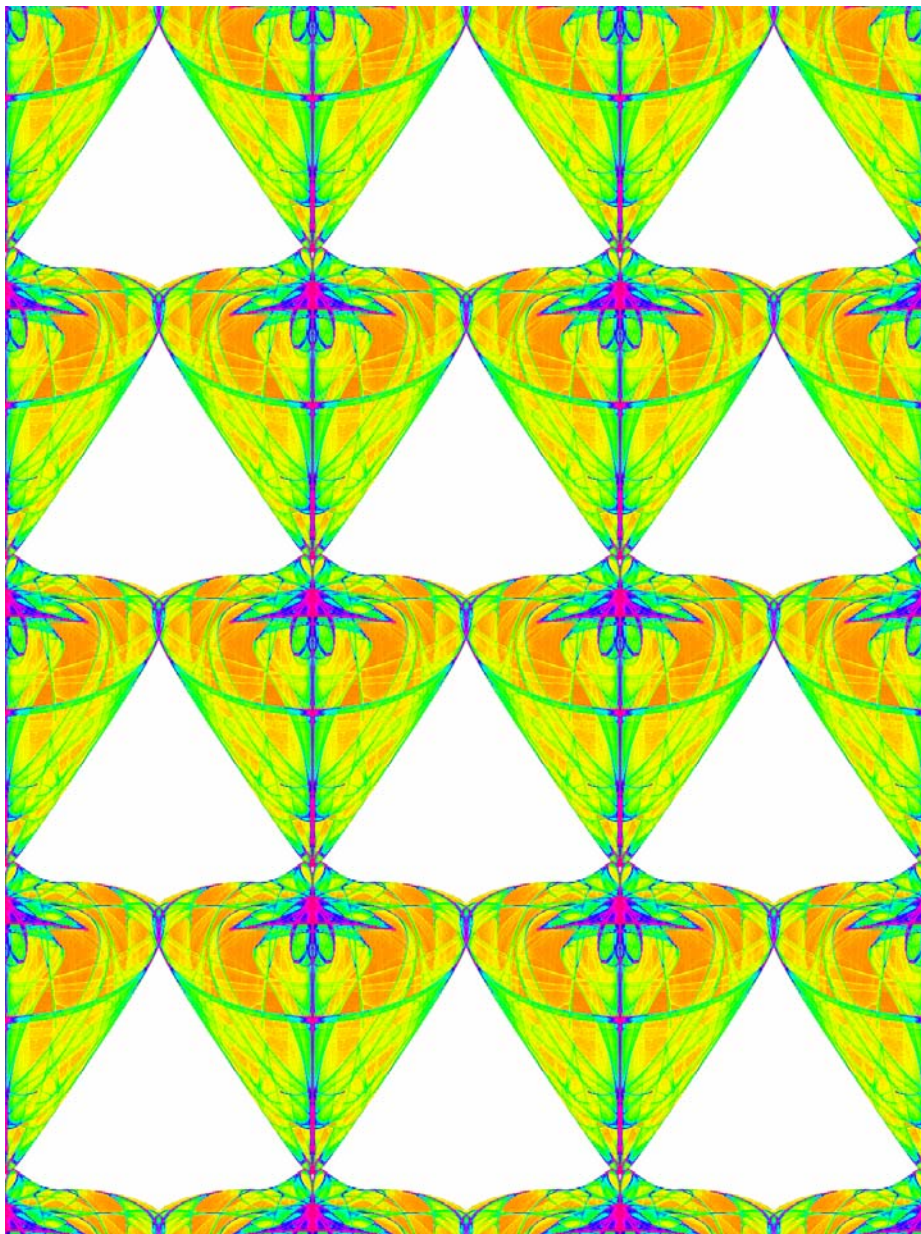


Figure 13: PM: An attractor with two translations and a reflection.

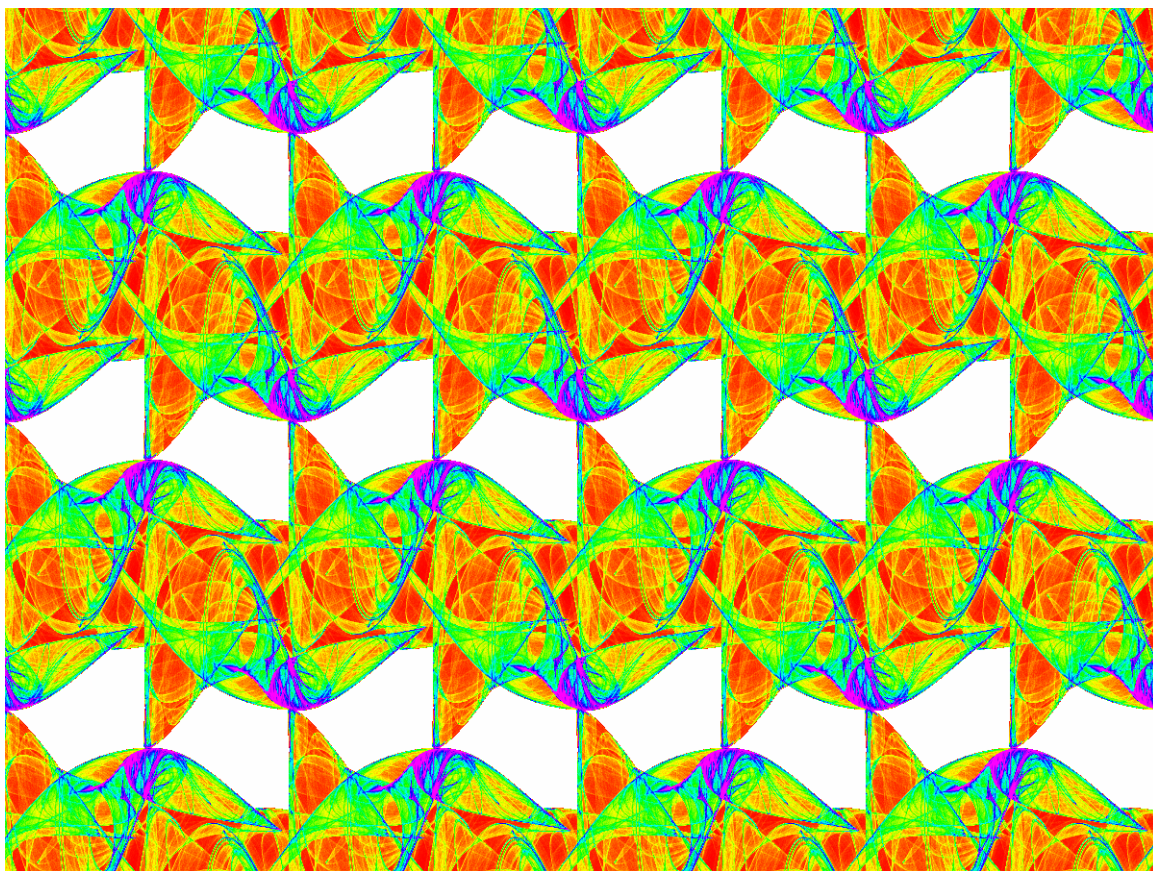


Figure 14: PG: An attractor with two translations and a glide reflection.

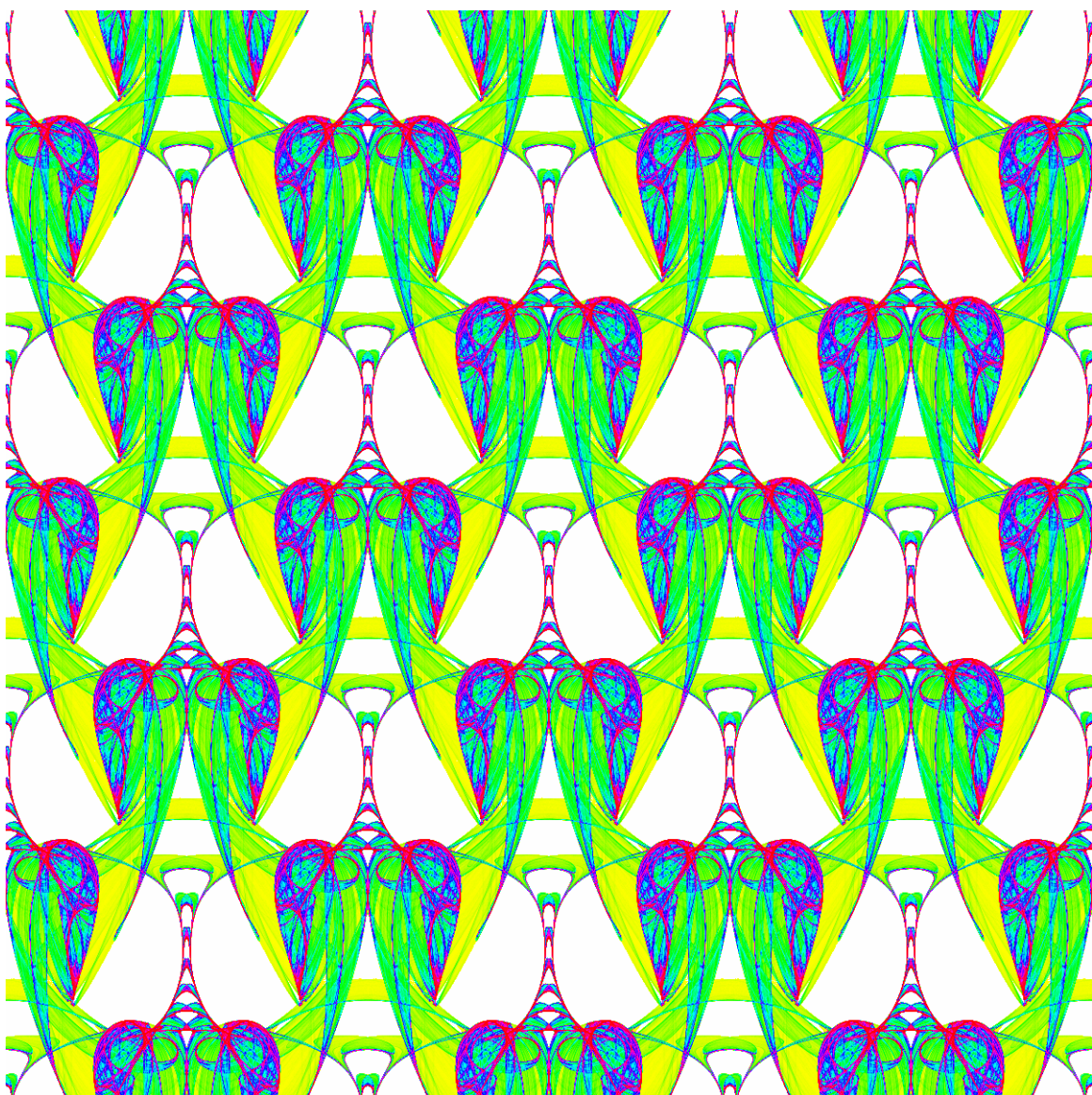


Figure 15: CM: An attractor with two translations and

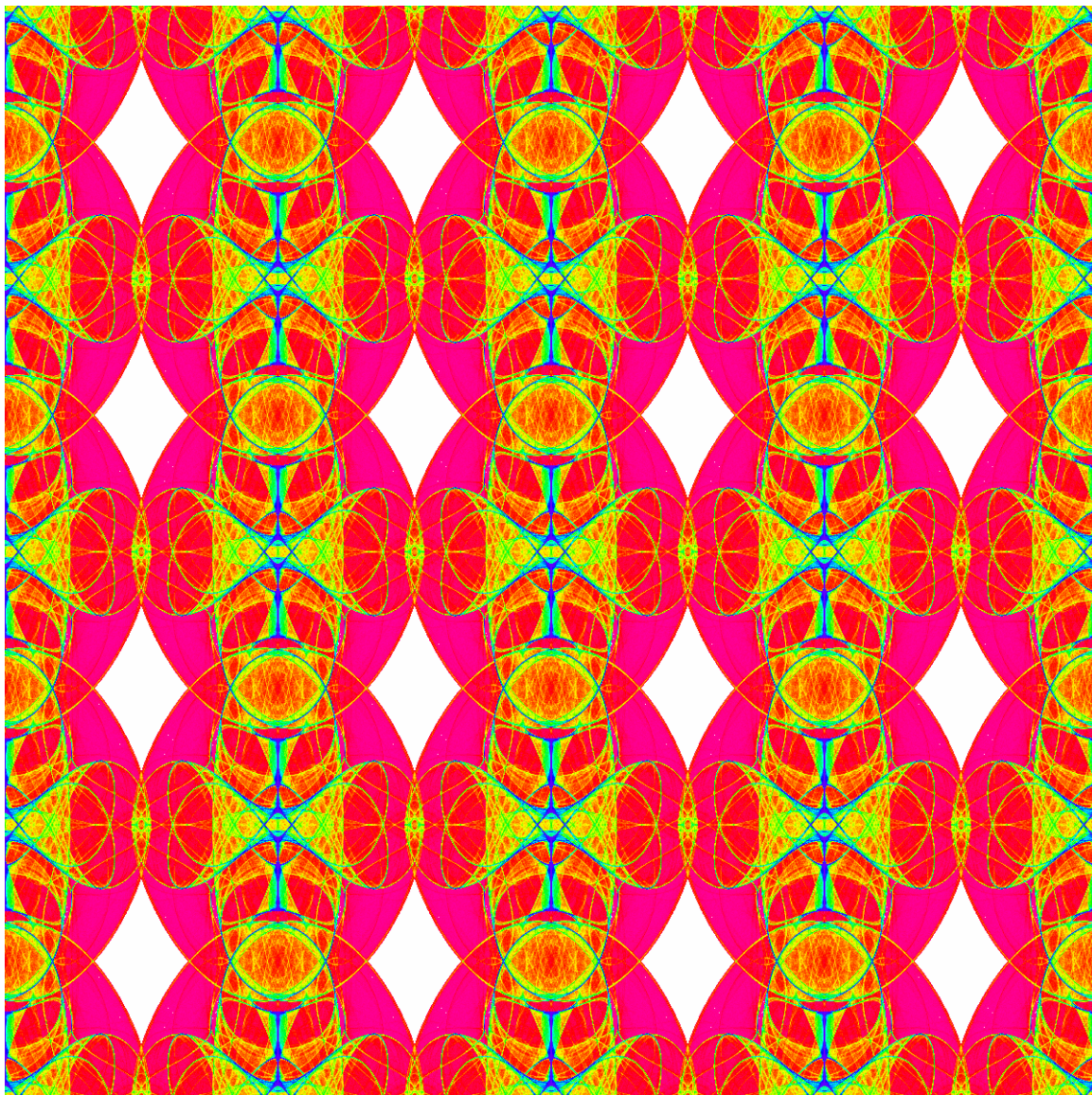


Figure 16: PMM: An attractor with two translations and two reflections.

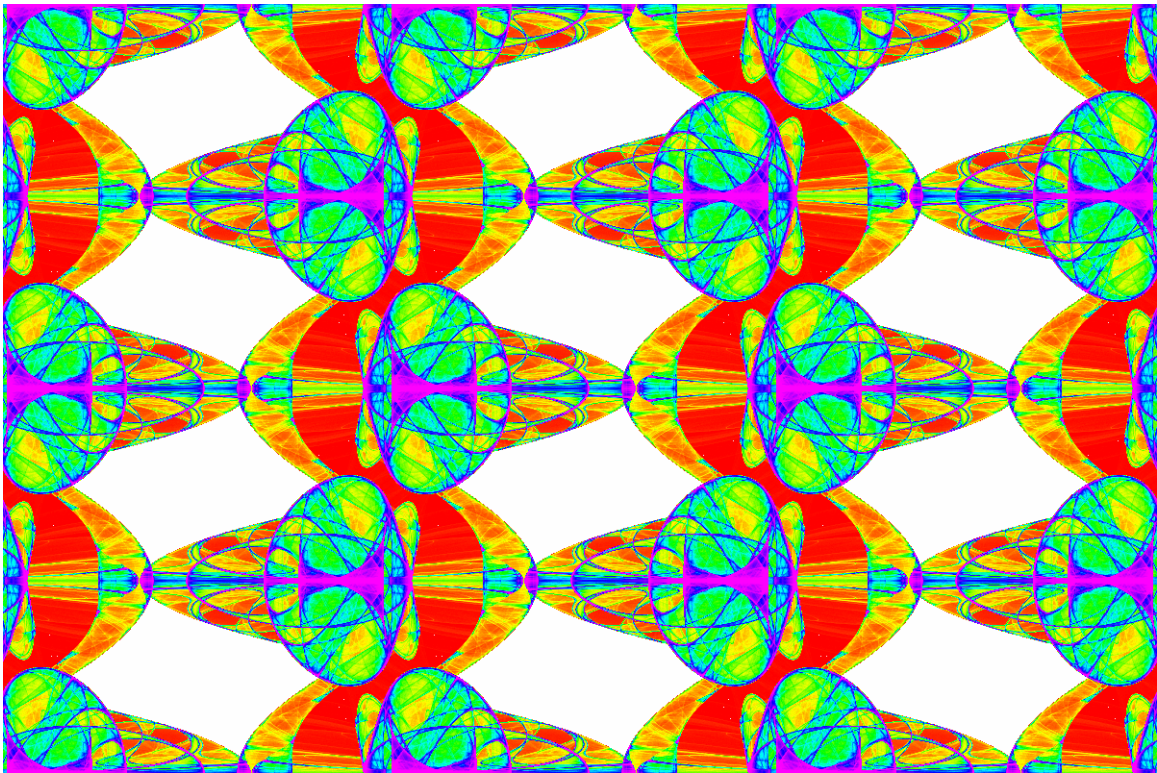


Figure 17: PMG: An attractor with two translations a reflection and a glide reflection.



Figure 18: PGG: An attractor with two translations and two glide reflections.

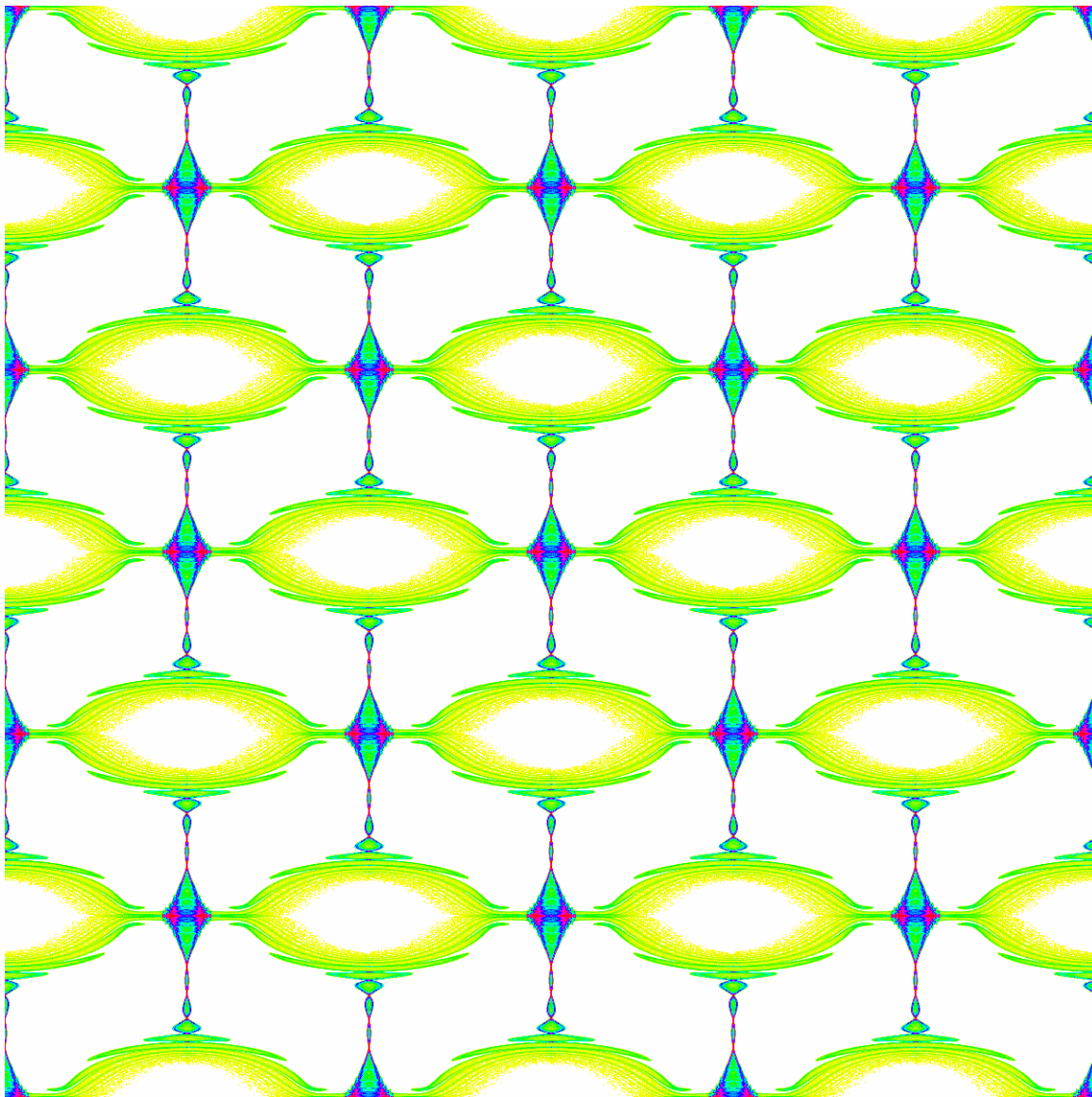


Figure 19: CMM: An attractor with two translations and

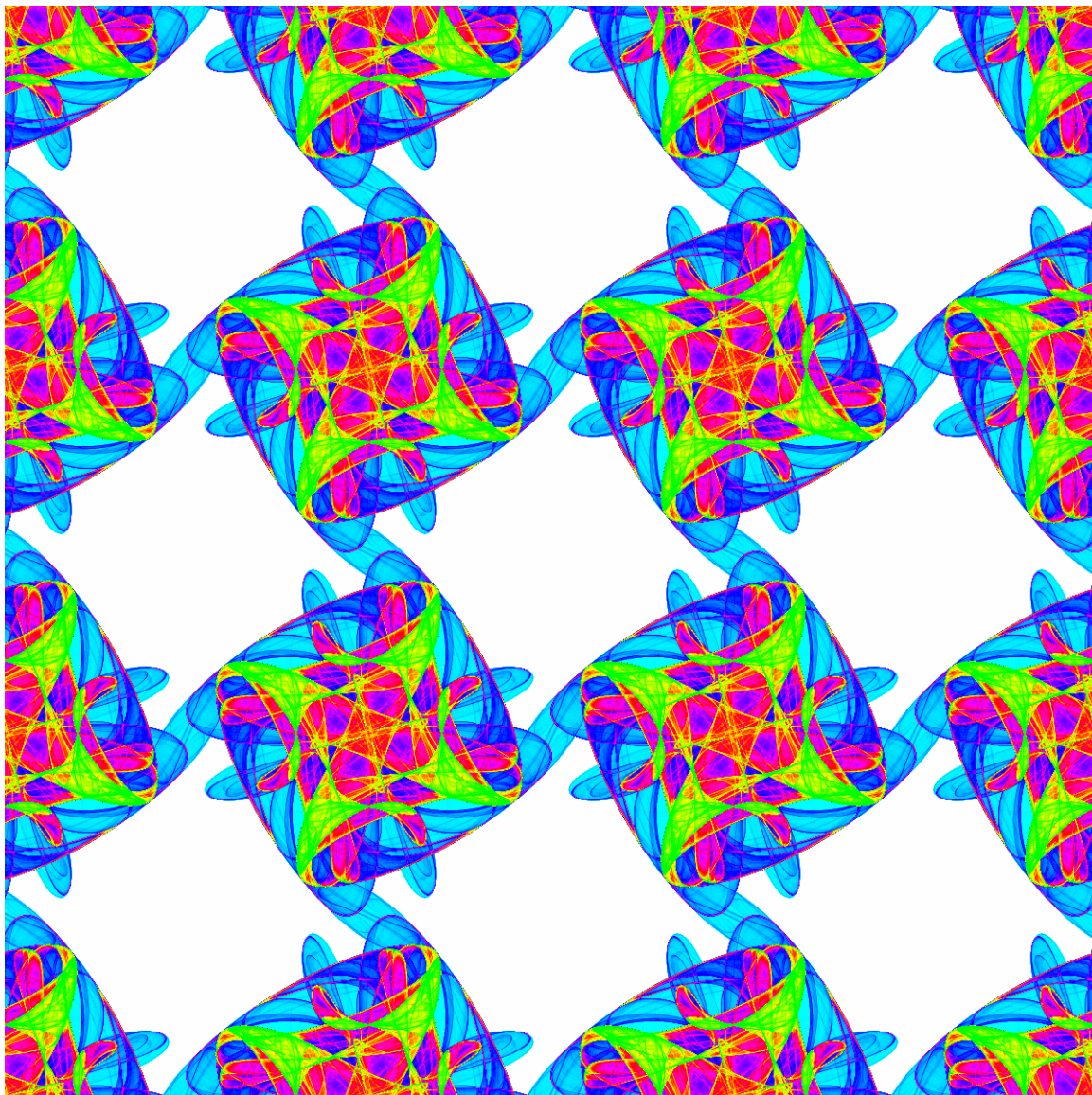


Figure 20: P4: An attractor with two translations and a quarter turn.

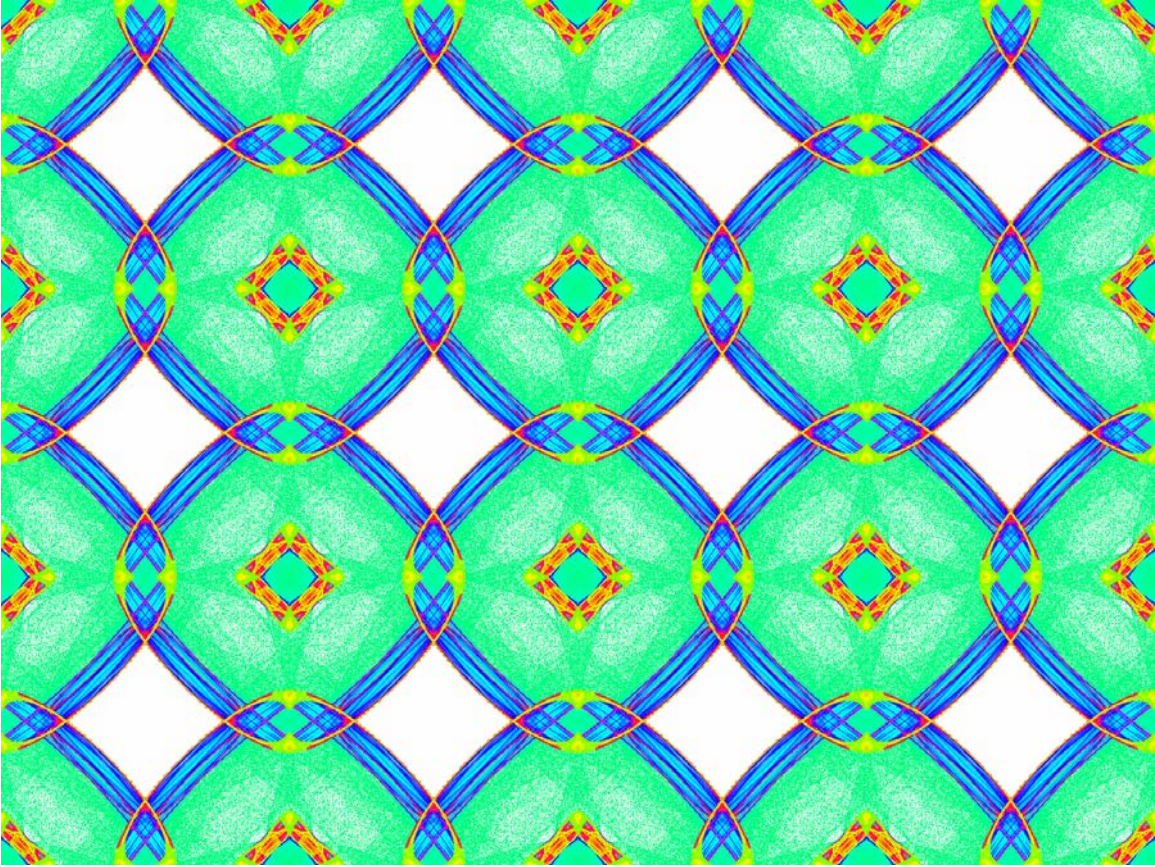


Figure 21: P4M: An attractor with two translations, a quarter turn and reflection.

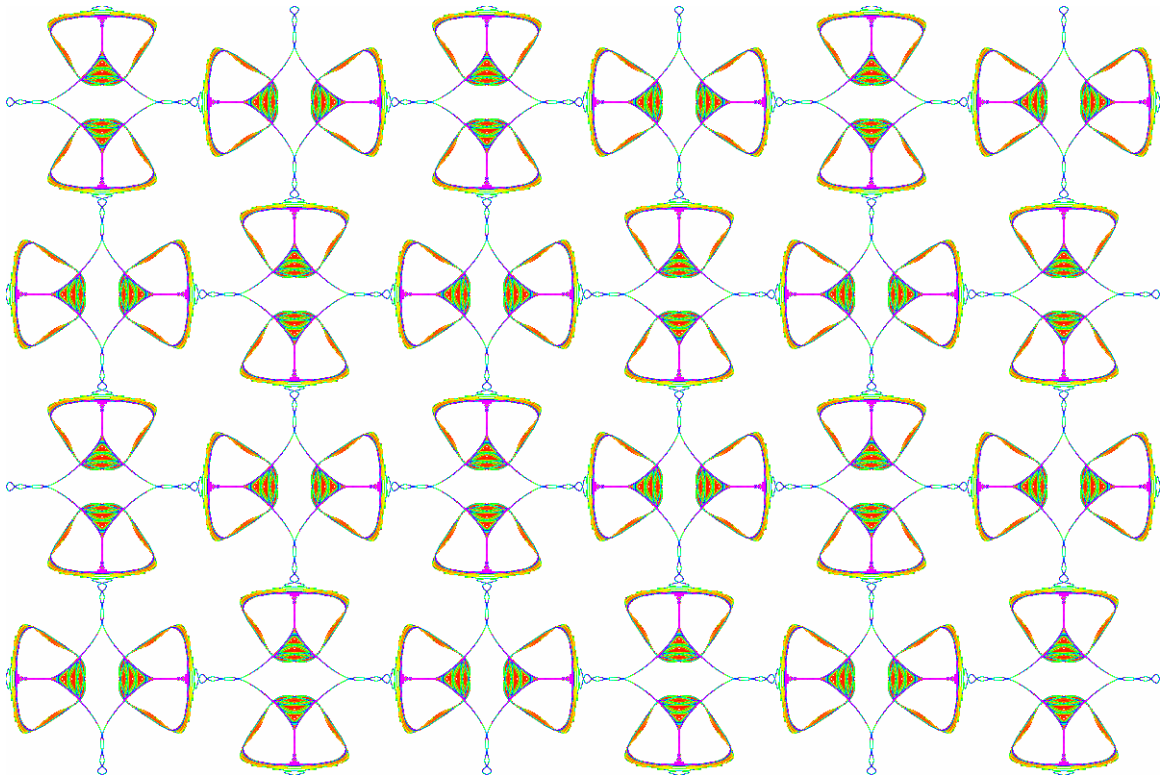


Figure 22: P4G: An attractor with glide reflections through quarter turns.

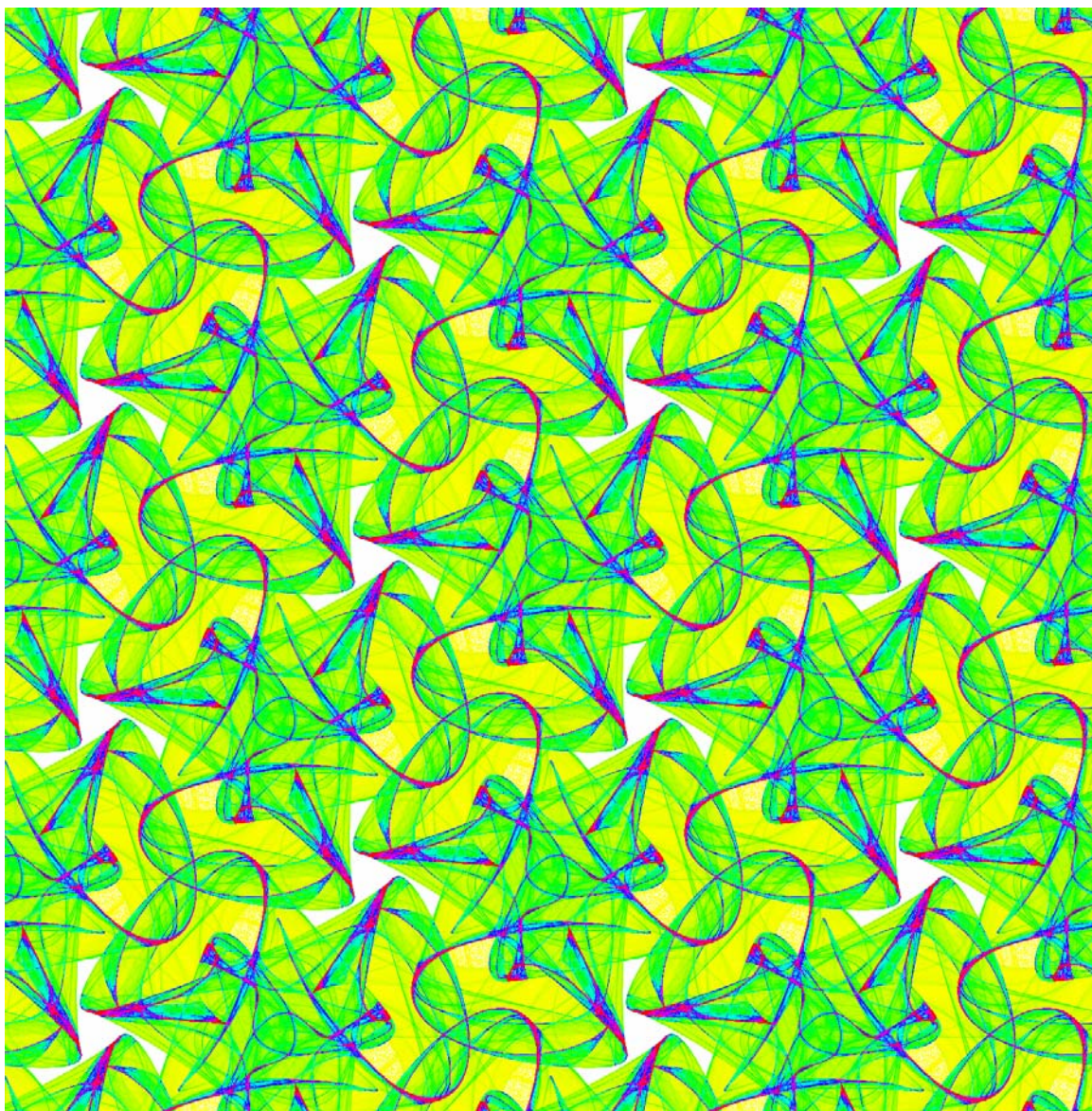


Figure 23: P3: An attractor with third turns.

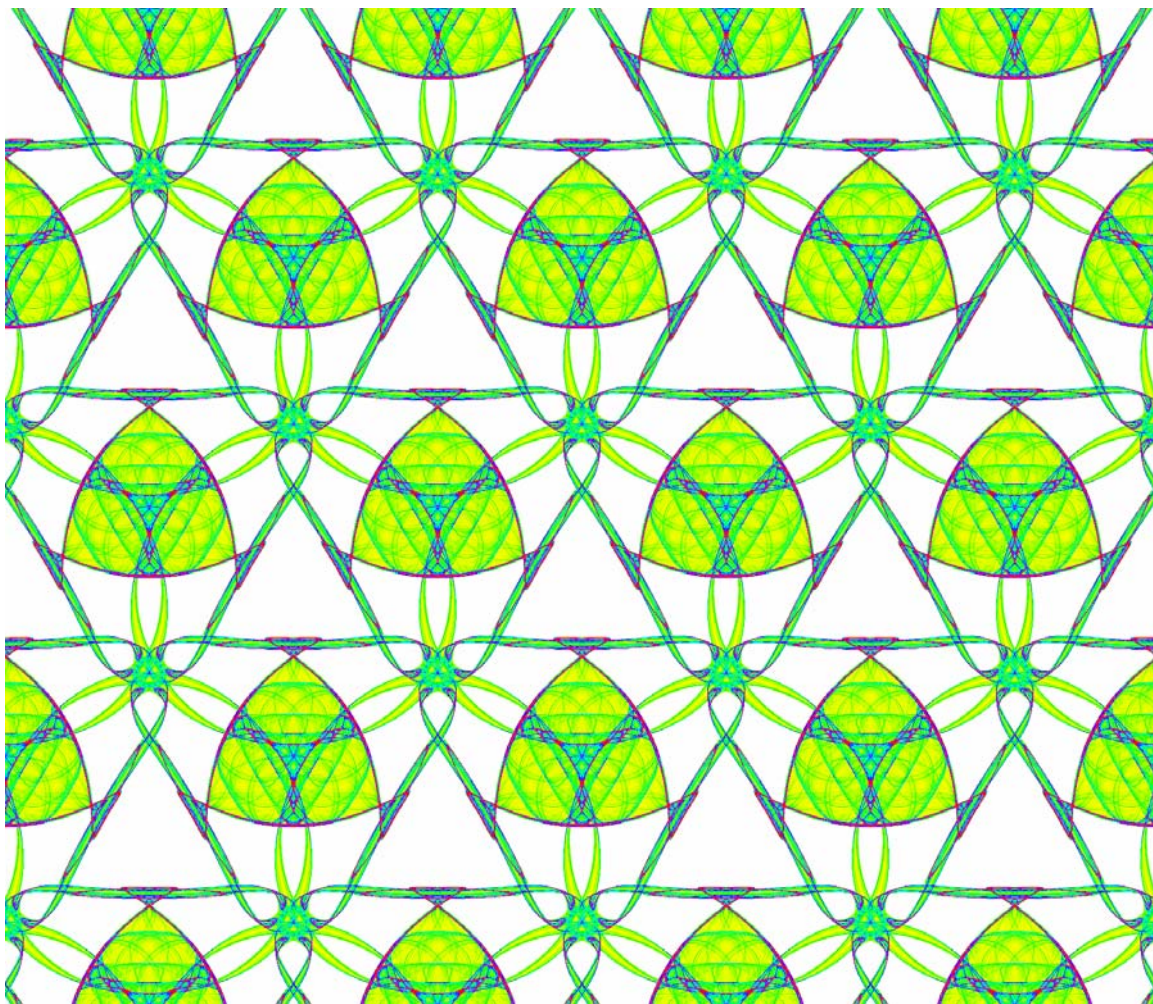


Figure 24: P3M1: An attractor with all third turns on reflections

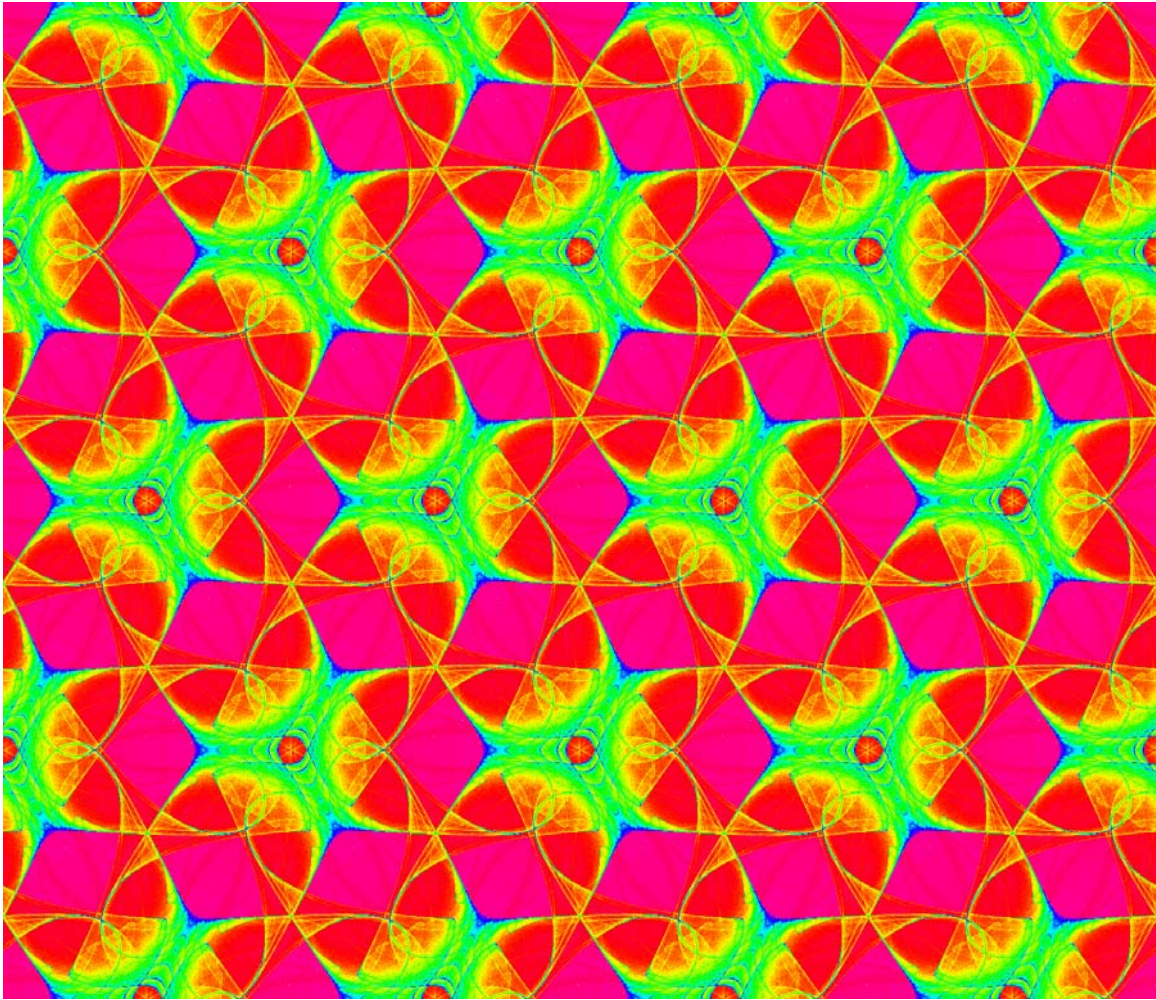


Figure 25: P31M: An attractor with some third turns on reflections.

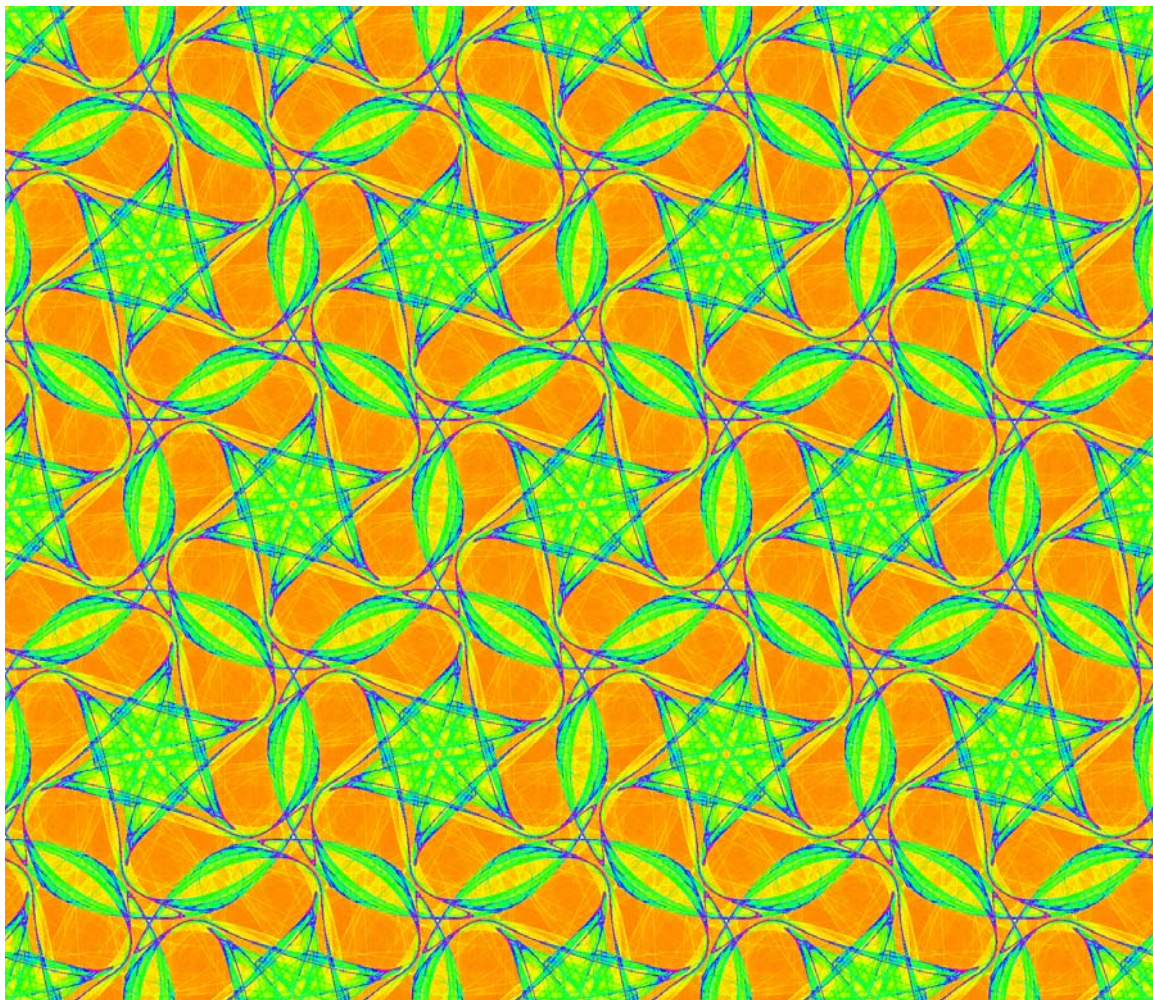


Figure 26: P6: An attractor with sixth turns.

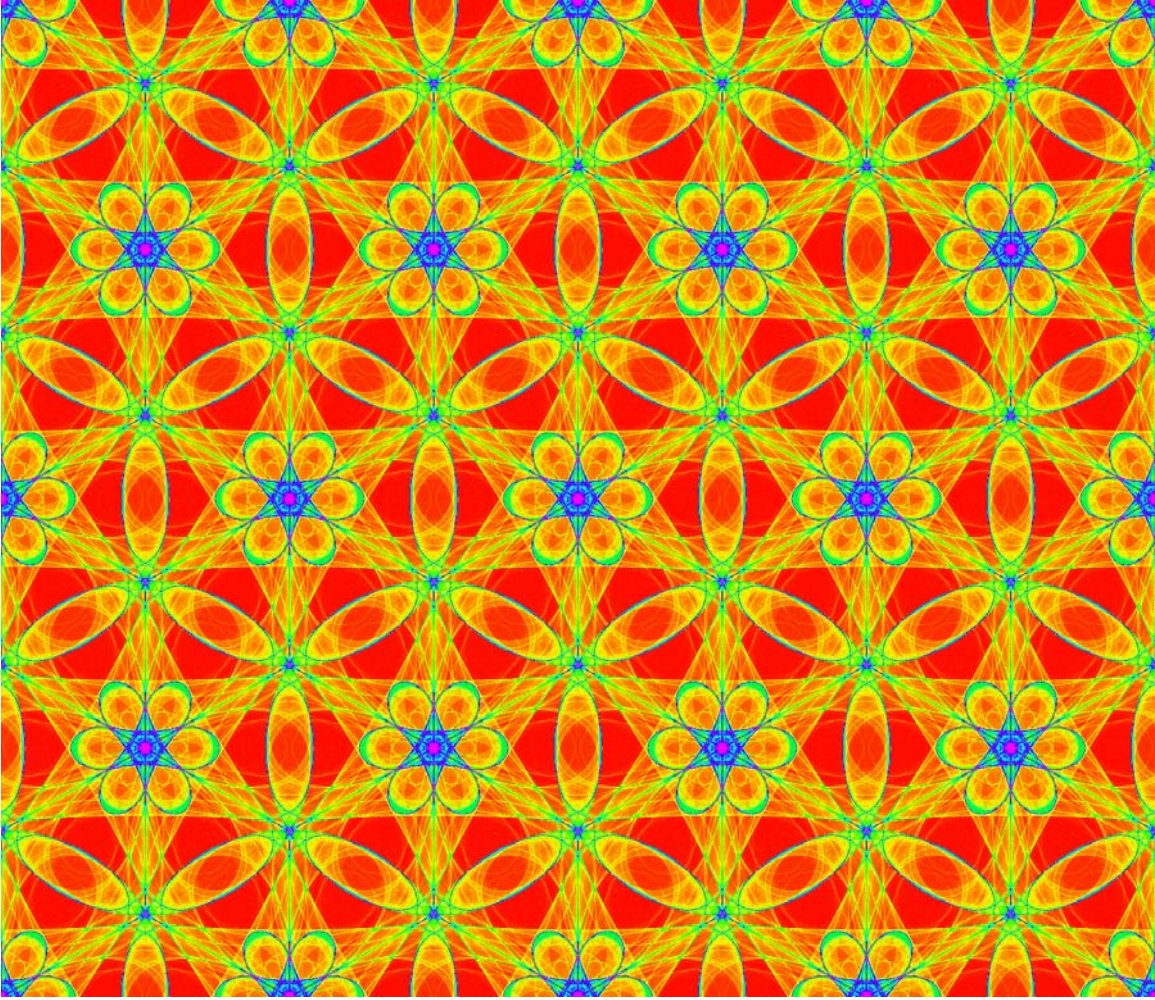


Figure 27: P6M: An attractor with reflections on sixth turns.